Article

Discovery of Potent and Selective PI3K# Inhibitors

Samuel L. Drew, Rhiannon Thomas-Tran, Joel W. Beatty, Jeremy Fournier, Kenneth V. Lawson, Dillon H. Miles, Guillaume Mata, Ehesan U. Sharif, Xuelei Yan, Artur K. Mailyan, Elaine Ginn, Jie Chen, Kent Wong, Divyank Soni, Puja Dhanota, Pei-Yu Chen, Stefan G. Shaqfeh, Cesar Meleza, Amber T. Pham, Ada Chen, Xiaoning Zhao, Jesus Banuelos, Lixia Jin, Ulrike Schindler, Matthew J. Walters, Stephen W. Young, Nigel P. Walker, Manmohan Reddy Leleti, Jay P. Powers, and Jenna L. Jeffrey

J. Med. Chem., **Just Accepted Manuscript** • DOI: 10.1021/acs.jmedchem.0c01203 • Publication Date (Web): 31 Aug 2020

Discovery of Potent and Selective PI3Kγ Inhibitors

*Samuel L. Drew, Rhiannon Thomas-Tran, Joel W. Beatty, Jeremy Fournier, Kenneth V. Lawson, Dillon H. Miles, Guillaume Mata, Ehesan U. Sharif, Xuelei Yan, Artur K. Mailyan, Elaine Ginn, Jie Chen, Kent Wong, Divyank Soni, Puja Dhanota, Pei-Yu Chen, Stefan G. Shaqfeh, Cesar Meleza, Amber T. Pham, Ada Chen, Xiaoning Zhao, Jesus Banuelos, Lixia Jin, Ulrike Schindler, Matthew J. Walters, Stephen W. Young, Nigel P. Walker, Manmohan Reddy Leleti, Jay P. Powers, and Jenna L. Jeffrey**

Arcus Biosciences, Inc., 3928 Point Eden Way, Hayward, California 94545, United States

Abstract

The selective inhibition of the lipid signaling enzyme PI3Kγ constitutes an opportunity to mediate immunosuppression and inflammation within the tumor microenvironment but is difficult to achieve due to the high sequence homology across the class 1 PI3K isoforms. Here, we describe the design of a novel series of potent PI3Kγ inhibitors that attain high isoform selectivity through the divergent projection of substituents into both the 'selectivity' and 'alkyl-induced' pockets within the ATP binding site of PI3Kγ. These efforts have culminated in the discovery of 5-[2-amino-3-(1-methyl-1*H*-pyrazol-4-yl)pyrazolo[1,5-*a*]pyrimidin-5-yl]-2-[(1*S*)-1-cyclopropylethyl]-7-(trifluoromethyl)-2,3-dihydro-1*H*-isoindol-1-one (**4**, IC_{50} = 0.064 μM, THP-1 cells), which displays >700-fold selectivity for PI3Kγ over the other class I isoforms and is a promising step towards the identification of a clinical development candidate. The structure-activity relationships identified throughout this campaign demonstrate that greater γ-selectivity can be achieved by inhibitors that occupy an 'alkyl-induced' pocket and possess bicyclic hinge-binding motifs capable of forming more than one hydrogen bond to the hinge region of PI3Kγ.

Introduction

The phosphoinositol-3-kinases (PI3Ks) constitute an integral part of a complex cell signaling network (including AKT and mTOR), which regulates many essential functions, such as cellular metabolism, growth, proliferation, and survival.[1,2] Oncogenic defects concerning this signaling network—both in the form of upstream over-activation and genetic alterations of its components[3]–embody many of the hallmarks

of cancer.[4, 5, 6] Early efforts to exploit these proteins as drug targets through the use of pan-isoform inhibitors of PI3K and dual-PI3K/mTOR inhibitors have been met with various challenges in the clinic, including inadequate efficacy and side effect profiles.[7] The class 1 family of PI3K signaling proteins has been the most intensively studied and consists of four isoforms (PI3Kα, PI3Kβ, PI3Kδ, and PI3Kγ).[8] PI3Kα and PI3Kβ are ubiquitous across many cell types, while PI3Kδ and PI3Kγ are limited in their expression, existing predominantly in leukocytes and garnering attention as potential therapeutic targets for the regulation of autoimmune and inflammatory disease, as well as cancer.[9, 10] Moreover, PI3Kγ plays an important and well-established role in regulating the differentiation and activation of myeloid-lineage immune cells, such as myeloid derived suppressor cells (MDSCs) and macrophages.[11]

Early success in selectively targeting a PI3K isoform in the context of oncology was realized in the discovery and approval of idelalisib (a PI3Kδ-selective inhibitor) for the treatment of relapsed chronic lymphocytic leukemia. In the treatment of solid tumors, functional inhibition of PI3Kγ in the tumor microenvironment (TME) may likewise have the potential to safely modulate the efficacy of immune-activating agents and influence disease progression.[12, 13] A high degree of tumor infiltration by MDSCs has been correlated with immune evasion, poor prognosis in human cancers, and serves as a negative predictive marker for single-agent immunotherapy regimens.[14, 15, 16] Consequently, PI3Kγ is an attractive and promising target for combination therapies to reverse immune evasion associated with chronic inflammation of the TME. Considering the therapeutic potential of PI3Kγ inhibition, we embarked on a medicinal chemistry campaign to identify a novel series of potent and isoform selective PI3Kγ inhibitors.

Our initial design plan was guided by a comparative assessment of known PI3Kγ inhibitors, including IPI-549 **3** (Infinity Pharmaceuticals)[17] and various chemotypes developed by Vertex Pharmaceuticals (benzothiazoles,[18] thiazolopiperidines,[19] and isoindolinones[20]), and AstraZeneca (aminothiazoles[21, 22]), as well as a plethora of published X-ray crystal structures of PI3Kγ complexes.[23] Several informative features emerged from an alignment of structurally disparate, enzyme-bound PI3Kγ inhibitors, including AZ2 **1**—a close analog of the more potent AZD-3458 (**2**, **Figure 1a**) in which the

isoindolinone methyl sulfone substituent is replaced by a methyl group—bound to mouse PI3Kδ (mPI3Kδ, PDB code 6FTN)[21, 22] and IPI-549 **3** (**Figure 1a**) in complex with human PI3Kγ (hPI3Kγ). Superposition of the two structures (**Figure 1b**) revealed striking differences in the binding modes of IPI-549 and AZ2: while the ligands share a common interaction with the hinge region, they largely occupy different pockets in and around the adenosine triphosphate (ATP) binding site of PI3K.

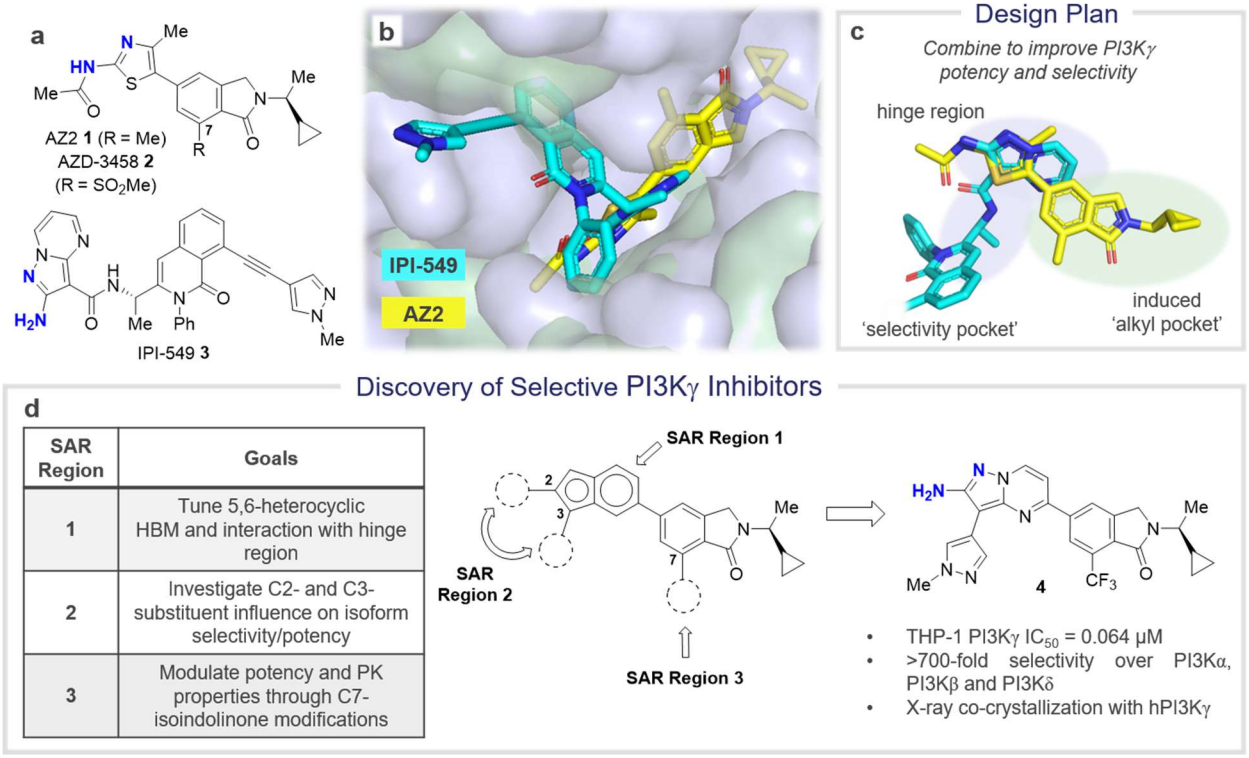

SAR Region	Goals
1	Tune 5,6-heterocyclic HBM and interaction with hinge region
2	Investigate C2- and C3-substituent influence on isoform selectivity/potency
3	Modulate potency and PK properties through C7-isoindolinone modifications

Figure 1. (a) Chemical structures of AZ2 (**1**), AZD-3458 (**2**) and IPI-549 (**3**), with the H-bond donor/acceptor atoms of the hinge-binding motif in blue. (b) Superposition of the X-ray crystal structures of human PI3Kγ (light blue) bound to **3** (PDB ID: 6XRL; **3** shown as a stick model and colored according to the atom type, with C in cyan, N in blue, and O in red) and mouse PI3Kδ (light green) complexed with **1** (C in yellow, N in blue, and O in red; PDB ID: 6FTN). X-Ray figures generated using Pymol™ v2.0.4, Schrödinger, LLC. (c) Design plan for PI3Kγ inhibitors. (d) SAR regions investigated during the discovery of selective PI3Kγ inhibitor **4**.

In the case of IPI-549, the high isoform selectivity likely results from differences among the PI3K isoforms around the 'selectivity pocket' of the ATP binding site.[17] It has been suggested that the alkyne substituent of IPI-549 may participate in unfavorable interactions with the non-conserved residue Thr750 of PI3Kδ (which corresponds to Lys802 in PI3Kγ) next to the selectivity pocket.[17] In contrast, the *N*-alkyl

isoindolinone group of AZ2 extends ~6.9 Å farther than the pyrazolopyrimidine group of IPI-549 and induces a new pocket adjacent to the ATP binding site (**Figure 1b**). AZ2 (**1**) reportedly achieves high isoform selectivity by inducing PI3Kγ-specific conformational changes in the DFG motif of the activation loop.[22]

Encouraged by the high isoform selectivity and divergent structural features of IPI-549 and AZ2, we initiated a medicinal chemistry campaign to design potent and selective inhibitors of PI3Kγ. Key to our design strategy was the unification of two fundamentally different mechanisms of selectivity, which would allow an inhibitor to achieve favorable interactions within both the ATP binding pocket and an adjacent alkyl-induced pocket of PI3Kγ (**Figure 1c**). Specifically, we hypothesized that tethering of the isoindolinone portion of **1** to a bicyclic hinge-binding motif (HBM) would invoke greater γ-selectivity by projecting the *N*-alkyl tail of the isoindolinone deeper into the 'alkyl pocket'. Incorporation of a 5,6-heterocyclic HBM would also enable a thorough exploration of structure-activity relationships (SAR) within three specific regions of chemical space, as outlined in **Figure 1d**. Described herein is the successful application of this approach, which led to the discovery of a novel series of potent and γ-selective PI3K inhibitors, including lead compound **4** (PI3Kγ IC_{50} = 0.064 μM, THP-1 cells) that has >700-fold selectivity over the other class 1 PI3K isoforms.

Results and Discussion

SAR

Initial SAR efforts looked to assess the viability of our design strategy and examined a wide range of bicyclic HBMs that contained at least one H-bond donor—for interaction with Val882—tethered to the *N*-alkyl isoindolinone scaffold of **1** (**Table 1**). Replacement of the aminothiazole HBM of **1** with a 2-aminobenzimidazole moiety produced (±)-**5**, which was inactive against all class 1 PI3K isoforms (IC_{50} > 10 μM), as determined in a coupled-enzyme biochemical assay that measures the propensity of test compounds to inhibit PI3K-mediated ADP generation (Promega's ADP-Glo Lipid Kinase Assay). Pleasingly, acetylation of the C2-amino group led to analog (±)-**6**, which showed selective inhibition of

PI3Kγ, albeit with modest activity (biochemical PI3Kγ IC_{50} = 482 nM). This observed impact of C2-substitution served as an early proof of concept. We hypothesized that the C2-acetamide group may allow for a bidentate hydrogen bonding interaction with Val882, in a similar vein to **1**. Incorporation of an additional nitrogen atom into the 5,6-bicycle (**7** and **8**) improved binding affinity in biochemical assays but led to reduced potency in a THP-1 cell assay, which assesses the capacity of test compounds to inhibit PI3Kγ-stimulated phosphorylation of endogenous AKT at serine residue 473. It is worth noting that many of the assayed compounds displayed a marked reduction in potency in the cellular assay format. This observed difference between biochemical and cellular potency is a well-recognized consequence of the inability of common biochemical assays to capture the complexity of live cells or account for differences in compound permeability, protein binding, and off-target engagement in the presence of more physiologically relevant concentrations of enzymes, transporters, and ATP.[24] Accordingly, for these initial SAR investigations, the THP-1 cell assay served as our primary indicator of inhibitor potency, while biochemical assays of PI3Kα, β, γ, and δ provided a higher throughput and robust measure of isoform selectivity.

In the case of triazolo-pyridines **7** and **8**, acetylation of the C2-amino group did not significantly impact affinity towards PI3Kγ. However, like the benzimidazole series, isomeric triazolo-pyridine (±)-**10**, with R^1 = NHAc, was more potent than its C2-amino congener (±)-**9**. We were delighted to find that incorporation of an imidazolopyridazine HBM bearing a C2-acetamide group led to a significant gain in potency across both biochemical and cellular assays (**12**, biochemical PI3Kγ IC_{50} = 5.5 nM, 87-fold improvement over **6**). Furthermore, analog **12** had exquisite isoform selectivity with no detectable inhibition of other class 1 PI3K isoforms (>1,800-fold selectivity). Consistent with previous trends, the C2-amino analog (±)-**11** was less potent than **12**. In addition to the promising potency and selectivity profile of **12**, we were enthused by the opportunity to incorporate additional substituents at C3 that would project farther into the 'selectivity pocket' and potentially allow for divergent SAR.

During concurrent investigations across a different series of PI3Kγ inhibitors, it was discovered that a *N*-methylpyrazole group was a suitable C3-substituent for projection into the 'selectivity pocket'.

Attachment of this motif onto the C3-position of the imidazolopyridazine core of **11** furnished analog **13** (**Series b, Table 1**) that had similar cellular potency to **12** and maintained high isoform selectivity. Somewhat surprisingly, when the C2-amino group was removed in the case of **14** (**Series b, Table 1**), leaving a sole H-bond acceptor for interaction with Val882, the compound was essentially equipotent to **13** towards PI3Kγ; however, this modification resulted in reduced isoform selectivity. This suggests that bicyclic HBMs capable of bidentate interaction with Val882 (and potentially Ala885) generally impart greater γ-selectivity than those with only a single H-bond acceptor capability when tethered to *N*-cyclopropylethyl isoindolinones.

Table 1. An initial assessment of bicyclic hinge-binding motifs paired with the isoindolinone scaffold.

Series a: R^2 = H Series b: R^2 = 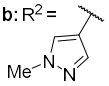 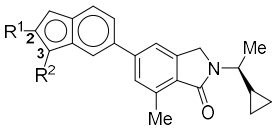				Biochemical IC_{50} (nM)[a,b]				THP-1 IC_{50} (μM)[a,b]
HBM	**Series**	R^1	**Analog**	**PI3Kγ**	**PI3Kα**	**PI3Kβ**	**PI3Kδ**	**PI3Kγ**
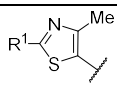	-		**1**[d]	3.6	3,900 (1,080x)	>10,000 (>2,750x)	1,780 (492x)	0.087
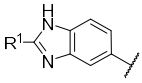	-		(±)-**5**	>10,000[c]	>10,000[c]	>10,000[c]	>10,000[c]	n.d.
	-		(±)-**6**	482	>10,000 (>21x)	>10,000 (>21x)	>10,000 (>21x)	1.0[c]
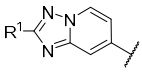	-		**7**	50	>10,000 (>198x)	>10,000 (>198x)	>10,000 (>198x)	3.1
	-		**8**	80	>10,000 (>125x)	>10,000 (>125x)	>10,000 (>125x)	3.9
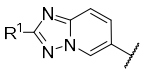	-		(±)-**9**	291	>10,000 (>35x)	>10,000 (>35x)	>10,000 (>35x)	15[c]
	-		(±)-**10**	76	>10,000 (>131x)	>10,000 (>131x)	>10,000 (>131x)	3.0
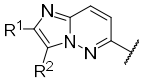	**a**		(±)-**11**	425	>10,000 (>24x)	>10,000 (>24x)	>10,000 (>24x)	1.5[c]
	a		**12**	5.5	>10,000 (>1,800x)	>10,000 (>1,800x)	>10,000 (>1,800x)	0.45
	b		**13**	17	>10,000 (>581x)	n.d.	>10,000 (>581x)	0.49[c]
	b		**14**	15[c]	4,240[c] (280x)	n.d.	2,380[c] (157x)	0.44
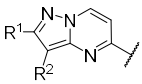	**a**		**15**	60	>10,000 (>167x)	n.d.	>10,000 (>167x)	4.2[c]
	a		**16**	4.4	>10,000 (>2,290x)	n.d.	>10,000 (>2,290x)	0.24
	b		**17**	2.9	>10,000 (>3,470x)	n.d.	>10,000 (>3,470x)	0.20
	b		**18**	429	>10,000 (>23x)	n.d.	>10,000 (>23x)	1.5[c]
	b		**19**	9.1[c]	4,140[c] (454x)	n.d.	3,440[c] (378x)	0.30

[a]Average of at least two measurements. [b]Numbers in parentheses indicate fold selectivity over PI3Kγ. [c]Single measurement obtained. [d]AZ2 **1** was prepared as described in the literature and was tested using Arcus' biochemical and cellular assays. Biochemical IC_{50} values determined using the ADP-Glo Lipid Kinase Assay (Promega) with 25 μM ATP and 50 μM enzyme substrate, phosphatidylinositol 4,5-bisphosphate. THP-1 IC_{50} values, determined using the AlphaLISA SureFire Ultra AKT 1/2/3

(pS473) Assay (PerkinElmer), reflect the capacity of test compounds to inhibit PI3Kγ-stimulated phosphorylation of endogenous AKT at serine 473. n.d. = value not determined.

Given the pyrazolopyrimidine HBM within **3** was optimal for selectivity and potency towards PI3Kγ, we anticipated that replacement of the imidazolopyridazine HBM with a pyrazolopyrimidine had the potential to invoke greater potency in our series of PI3Kγ inhibitors. Indeed, transitioning from **12** to **16** (R^1 = NHAc, **Series a, Table 1**) yielded a roughly 2-fold improvement in cellular potency (**16**, PI3Kγ IC_{50} = 0.24 μM, THP-1 cells) and importantly, pyrazolopyrimidine **16** showed no appreciable binding across PI3Kα and PI3Kδ biochemical assays. In a similar vein to the imidazolopyridazine series, the C2-amino pyrazolopyrimidine **15** that lacked a C3-substituent was less potent, but potency returned upon incorporation of a *N*-methylpyrazole group at C3 (**17**, THP-1 PI3Kγ IC_{50} = 0.20 μM). In comparing the activity of compound **18** to **17** (**Series b, Table 1**) there is a clear preference for $R^1 = NH_2$ versus R^1 = NHAc when C3 is substituted; however, R^1 = H (**19**) is also tolerated at the cost of isoform selectivity. Pyrazolopyrimidine **17** displayed promising pharmacokinetic (PK) properties with a low intrinsic clearance in human and rat hepatocytes, which correlated well with *in vivo* measurements in rats; however, compound **17** was a potent CYP3A4 inhibitor and demonstrated CYP3A4 time-dependent inhibition (TDI) (**Figure 2**).

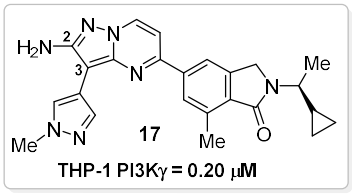

PK Properties

Cl_{int} (μL/min/10^6 cells)	
human	rat
3.8	2.9
Rat CL (L/hr/kg) = 1.34	

CYP Profile

CYP Inhibition IC_{50} (μM)				
1A2	2D6	2C9	2C19	3A4
>40	>40	2.4	3.7	0.45

CYP3A4 TDI
%activity loss at 10 μM = 67%

Figure 2: PK properties and CYP inhibition profile of pyrazolopyrimidine **17**.

Having identified several new structural classes of promising lead PI3Kγ inhibitors, we commenced a second phase of SAR optimization and characterization to further improve potency, selectivity, and PK properties. Efforts to confer additional binding affinity through modification of the C2-acetamide group in

the imidazolopyridazine series were largely unsuccessful (**Table 2**). Extension of the acetamide alkyl chain (e.g., **20**-**22**), incorporation of a phenyl group (**23**), or replacement of the acetamide group with a methylsulfonamide (**24**) led to a significant or complete erosion of potency towards PI3Kγ.

Table 2. Investigation of C2-substitution in imidazolopyridazine series lacking C3-substituents.

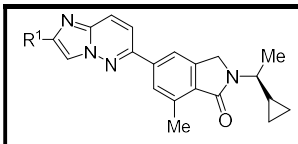		Biochemical IC_{50} (nM)[a,b]				THP-1 IC_{50} (μM)[a,b]
R^1	**Analog**	**PI3Kγ**	**PI3Kα**	**PI3Kβ**	**PI3Kδ**	**PI3Kγ**
	**12**	5.5	>10,000 (>1,800x)	>10,000 (>1,800x)	>10,000 (>1,800x)	0.45
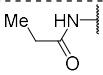	**20**	7.3	>10,000 (>1,370x)	n.d.	>10,000 (>1,370x)	0.83
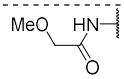	**21**	14	>10,000 (>710x)	n.d.	>10,000 (>710x)	0.69
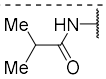	**22**	70	>10,000 (>142x)	n.d.	>10,000 (>142x)	9.4[c]
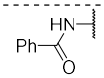	**23**	93	>10,000 (>107x)	n.d.	>10,000 (>107x)	12[c]
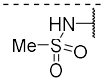	**24**	5,300	>10,000 (>1.9x)	n.d.	>10,000 (>1.9x)	>30[c]
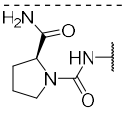	**25**	2.9	2,470 (839x)	n.d.	8,210 (2,790x)	0.46

[a]Average of at least two measurements. [b]Numbers in parentheses indicate fold selectivity over PI3Kγ. [c]Single measurement obtained. n.d. = value not determined.

Integration of an (*S*)-pyrrolidine carboxamide moiety, which was a structural feature key to the discovery of PI3Kα inhibitor BYL719 (alpelisib),[25] furnished compound **25** (PI3Kγ IC_{50} = 0.46 μM, THP-1 cells), which was equipotent to the parent acetamide **12**. In the case of BYL719, the (*S*)-pyrrolidine carboxamide group is proposed to impart PI3Kα selectivity via two H-bonding interactions with the side chain amide of a non-conserved residue (Q859) within the ATP binding pocket of PI3Kα. Our observations suggest that these favorable interactions with Q859 of PI3Kα are not enough to overcome the PI3Kγ-selective influence of the *N*-cyclopropylethyl isoindolinone in **25** that projects into the 'alkyl pocket' near the DFG motif. As no significant improvements in potency were realized through these modifications to

the hinge region, focus was directed towards isoindolinone modifications (**SAR region 3, Figure 1d**) and variation of C3 pyrazolopyrimidine substituents (**SAR region 2, Figure 1d**), stemming from lead PI3Kγ inhibitor **17**.

Table 3: C3-Substitution SAR in the pyrazolopyrimidine series.

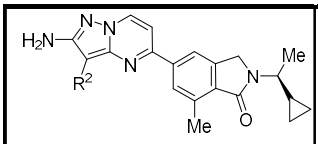		Biochemical IC_{50} (nM)[a,b]				THP-1 IC_{50} (μM)[a,b]
R^2	Analog	PI3Kγ	PI3Kα	PI3Kβ	PI3Kδ	PI3Kγ
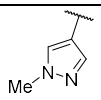	**17**	2.9	>10,000 (>3,470x)	n.d.	>10,000 (>3,470x)	0.20
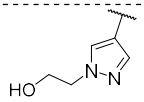	**26**	6.4[c]	1,160[c] (213x)	n.d.	1,160[c] (213x)	0.40
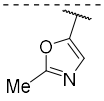	**27**	5.9[c]	2,260[c] (385x)	n.d.	3,250[c] (554x)	0.23
	**28**	44[c]	1,980[c] (45x)	n.d.	2,690[c] (61x)	0.62
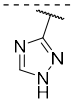	**29**	31[c]	6,290[c] (212x)	n.d.	6,050[c] (196x)	0.63
	**30**	64[c]	>10,000 (>156x)	n.d.	>10,000 (>156x)	2.3[c]
	**31**	7.5[c]	2,730[c] (362x)	n.d.	2,200[c] (292x)	0.55
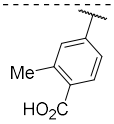	**32**	2.2	96.0 (42x)	n.d.	210 (91x)	0.21
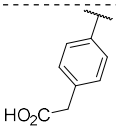	**33**	2.1	5,450 (2,550x)	n.d.	4,660 (2,180x)	0.87

[a]Average of at least two measurements. [b]Numbers in parentheses indicate fold selectivity over PI3Kγ. [c]Single measurement obtained. n.d. = value not determined.

A series of aryl and heteroaryl C3-modifications was evaluated following the discovery of *N*-methylpyrazole **17**. In an attempt to improve potency and mitigate CYP inhibition liabilities by reducing

lipophilicity, the *N*-methyl group of **17** (predicted logD = 3.29 [ChemAxon]) was replaced with a hydroxyethyl moiety (**26**, **Table 3**, predicted logD = 2.60). This modification was poorly tolerated and resulted in a two-fold reduction in PI3Kγ cellular potency, along with an erosion of isoform selectivity against PI3Kα and PI3Kδ (>3,470-fold → 213-fold, biochemical). Oxazole **27** retained similar cellular activity compared to **17** but suffered from poor stability in rat hepatocytes (Cl_{int} = 22.4 μL/min/10^6 cells). Alternative 5-membered heterocycles, such as pyrazoles (**28**) and triazoles (**29**) led to a 3-fold loss in cellular activity, while a 2-pyridinyl substituent (**30**) rendered an 11-fold reduction in cellular PI3Kγ inhibition. Relative to pyridine **30**, pyrimidine **31** was 4-fold more potent (cellular assay), but still 2-fold less active than lead C3-pyrazole **17**.

In concurrent studies, *para*-benzoic acids flanked by *ortho*-alkyl groups were identified as promising C3-substitutents and attachment of a similar moiety to the pyrazolopyrimidine scaffold furnished analog **32**. Although *para*-benzoic acid **32** had comparable potency to pyrazole **17**, isoform selectivity was eroded, and the compound was <100-fold selective against PI3Kα and PI3Kδ. Homologation of the *para*-benzoic acid moiety to a *para*-phenylacetic acid group (**33**) resulted in improved isoform selectivity in biochemical assays but a 4-fold loss of potency in the PI3Kγ cellular assay relative to **32**. Although these investigations did not lead to a significant improvement in the potency of our γ-selective PI3K inhibitors, our observations suggested that placement of *para*-benzoic acid groups at the C3-position of the pyrazolopyrimidine HBM might provide an avenue for further optimization and avoidance of the CYP liabilities likely associated with the C3 *N*-methylpyrazole moiety (*vide infra)*.

During the discovery of **2**, it was shown that replacement of the C7-methyl substituent of the isoindolinone within **1** with polar sulfonamide groups influenced the binding affinity and PK properties of PI3Kγ inhibitors bearing the *N*-cyclopropylethyl tail.[21] As such, we investigated modifications at this position within our lead pyrazolopyrimidine series and discovered that nitrogen- and sulfur-linked methylsulfonamides (**35** and **36**, respectively), as well as a C7-trifluoromethyl group (**34**) conferred a significant improvement in biochemical and/or cellular potency relative to **16**, while maintaining exquisite isoform selectivity.

Table 4: C7-Isoindolinone Modifications.

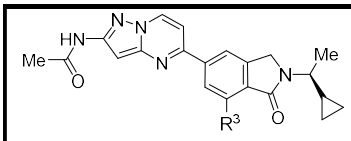		Biochemical IC_{50} (nM)[a,b]				THP-1 IC_{50} (μM)[a,b]
R^3	**Analog**	**PI3Kγ**	**PI3Kα**	**PI3Kβ**	**PI3Kδ**	**PI3Kγ**
	**16**	4.4	>10,000 (>2,290x)	n.d	>10,000 (>2,290x)	0.24
	**34**	2.2	8,340 (3880x)	n.d.	2,610 (1210x)	0.15
	**35**	1.3	8,970 (7,060x)	n.d.	6,140 (4,840x)	0.16
	**36**	2.7	9,850 (3,590x)	n.d.	4,550 (1,660x)	0.24[c]

[a]Average of at least two measurements. [b]Numbers in parentheses indicate fold selectivity over PI3Kγ. [c]Single measurement obtained. n.d. = value not determined.

In addition, compound **34** (PI3Kγ IC_{50} = 0.15 μM, THP-1 cells) bearing a C7-CF_3 group, which was the most potent compound in cellular assays, was shown to have low intrinsic clearance in both rat and human hepatocytes, and demonstrated a favorable direct CYP inhibition profile, with negligible CYP3A4 TDI (**Table 6**). Having identified an avenue for further potency gains, we took advantage of our general PI3Kγ inhibitor design and reexamined the SAR vector off the pyrazolopyrimidine C3-position in combination with the promising C7-CF_3 isoindolinone modification.

To our delight, amalgamation of the C7-CF_3 isoindolinone with the previously discovered C3-*N*-methylpyrazole amino-pyrazolopyrimidine HBM rendered a 3-fold improvement in cellular potency (**4**, PI3Kγ IC_{50} = 0.064 μM, THP-1 cells, **Table 5**). Compound **4** displayed a promising isoform selectivity profile (1,040-fold selective over PI3Kα and 700-fold selective over PI3Kδ) with no appreciable binding to PI3Kβ. Additional characterization showed that lead **4** had a low intrinsic clearance in human and rat hepatocytes, which correlated well with intravenous dosing in rats where a low clearance was observed; however, similar to compound **17**, **4** was a potent CYP3A4 inhibitor and demonstrated CYP3A4 TDI (**Table 6**).

Table 5: Cumulative optimization across SAR regions 1-3 and identification of lead compounds **4** and **41**.

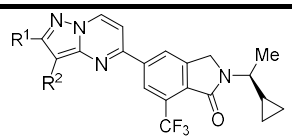			Biochemical IC_{50} (nM)[a,b]				THP-1 IC_{50} (μM)[a,b]
R^2	R^1	Analog	PI3Kγ	PI3Kα	PI3Kβ	PI3Kδ	PI3Kγ
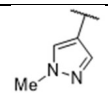	H_2N—	**4**	1.9	1,940 (1,040x)	>15,000[c]	1,310 (700x)	0.064
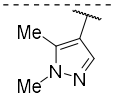	H_2N—	**37**	6.6[c]	1,510[c] (246x)	n.d.	2,240[c] (367x)	0.44
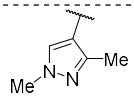	H_2N—	**38**	8.0[c]	>10,000[c] (>1,250x)	n.d.	4,550[c] (570x)	0.47
	H_2N—	**39**	53[c]	>10,000[c] (>190x)	n.d.	>10,000[c] (>190x)	0.80
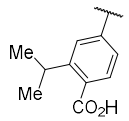	H_2N—	**40**	1.0	82.4 (82x)	10,100[c] (10,100x)	125 (125x)	0.076
	H—	**41**	2.1	194[c] (92x)	11,600[c] (5,530x)	459[c] (218x)	0.074

[a]Average of at least two measurements. [b]Numbers in parentheses indicate fold selectivity over PI3Kγ. [c]Single measurement obtained. n.d. = value not determined.

In an attempt to mitigate the CYP liabilities of lead **4**, methyl groups were incorporated adjacent to the pyrazole nitrogens of **4**, but this was poorly tolerated and yielded a roughly 7-fold loss in cellular potency towards PI3Kγ (**37** and **38**). Replacement of the C3-pyrazole with a pyrimidine substituent (**39**) also reduced cellular potency, but in this case CYP3A4 TDI (%activity loss at 10 μM = 17%) was reduced. Building on the previous realization that *para*-benzoic acids were suitable C3-pyrazole replacements, we evaluated the effect of incorporating sterically bulky substituents, such as isopropyl groups, *ortho* to the carboxylic acid group. Pleasingly, benzoic acid **40** had similar cellular potency (PI3Kγ IC_{50} = 0.076 μM, THP-1 cells) to pyrazole **4** and retained moderate selectivity over PI3Kα and PI3Kδ, with >10,000-fold selectivity over PI3Kβ. Finally, removal of the C2-amino group from the HBM (in a similar vein to **17**→**19**) afforded acid **41** that was equipotent to **40** and maintained a comparable selectivity profile against the class 1 PI3K isoforms. Acid **41** was stable to human and rat hepatocytes; however, this compound demonstrated

supra-hepatic clearance when dosed intravenously in rats during preliminary experiments. Pleasingly, this modification to the HBM in union with the C3-benzoic acid moiety significantly mitigated CYP3A4 TDI liabilities (**Table 6**).

This SAR campaign demonstrated the utility of combining *N*-cyclopropylethyl isoindolinone moieties, which enable 'alkyl pocket' inducement, with hetero-bicyclic HBMs that allow C3-substitution and extension into the 'selectivity pocket' of PI3Kγ. The SAR investigations described herein did not ultimately identify a compound suitable for further progression towards clinical development and thus precluded a more thorough characterization of the functional activity and selectivity of these inhibitors, e.g., against a broad panel of kinases. Nevertheless, these studies provided clear validation of our design strategy and resulted in the discovery of several lead compounds, setting the stage for further optimization towards the development of more potent and selective PI3Kγ inhibitors. Importantly, we were able to gain valuable insights into the factors that influence both potency and selectivity of PI3Kγ inhibitors through X-ray co-crystallization of structurally distinct inhibitors **3** and **4** with hPI3Kγ.

Table 6: Pharmacokinetic and CYP properties of lead PI3Kγ inhibitors.

Analog	Hepatocyte Cl_{int} (μL/min/10^6 cells)[a]		Rat Pharmacokinetic Data (IV)			CYP Inhibition IC_{50} (μM)[b]					CYP3A4 TDI
	Human	Rat	Dose (mg/kg)	CL (L/h/kg)	V_{ss} (L/kg)	1A2	2D6	2C9	2C19	3A4	%activity loss[c]
17	3.8	2.9	0.25	1.3	1.7	>40	>40	2.4	3.7	0.45	67
34	2.4	<1.2	n.d.	n.d.	n.d.	>40	>40	>40	12	4.6	12
4	3.3	7.4	0.25	0.78	1.2	7.5	>40	>40	12	0.60	77
41	<1.2	1.7	0.25	5.2	25	n.d.	n.d.	n.d.	n.d.	n.d.	13

[a]Single *in vitro* hepatocyte stability measurements. [b]CYP inhibition values refer to single experiment IC_{50} determinations. [c]CYP3A4 TDI refers to %activity loss at 10 μM and is a single measurement. n.d. = value not determined. Predicted LogD values (ChemAxon): **4** (3.65), **17** (3.29), **34** (3.64) and **41** (3.07).

X-Ray Co-Crystallization

As depicted in **Figure 3a**, IPI-549 **3** binds to the active site of hPI3Kγ in a conformation reminiscent of other 'propeller-shaped' PI3K inhibitors,[26] such as PIK-39 (PDB ID 2WXF)[27] and idelalisib (PDB ID

4XE0),[28] many of which exhibit selectivity for PI3Kδ over the other PI3K isoforms. Specifically, the ligand adopts a twisted orientation, with a 92.2° angle between the plane of the quinazolinone core and the aminopyrazolopyrimidine amide moiety, the planarity of which is reinforced by two intramolecular H-bonds. The plane of the *N*-phenyl substituent is also orthogonal to the plane of the quinazolinone. In addition to two specific H-bonds between the aminopyrazolopyrimidine and the backbone atoms of Val882, the quinazolinone moiety of IPI-549 interacts with the indole ring of Trp812 via edge-to-face π-stacking (**Figure 3b**).

Figure 3c depicts the binding geometry of lead compound **4** in complex with hPI3Kγ. Consistent with our hypothesis and the design plan outlined in Figure 1, **4** binds to the active site of hPI3Kγ in a manner analogous to the reported crystal structure of *N*-alkylisoindolinone **1** in complex with mPI3Kδ (PDB ID 6FTN). Similar to **1**-mPI3Kδ, the isoindolinone *N*-alkyl group of **4** projects into an induced pocket next to the affinity pocket (Figure 3d), the formation of which is accompanied by a shift in the position of the DFG motif.[21, 22] The contiguous aromatic rings of **4** adopt a mostly flat conformation within the active site, with the outer edge of the aminopyrazolopyrimidine group positioned 3.8 Å away from the side chain of Ile879 (not shown, for clarity), which contributes to the surface of the affinity pocket and may be analogous to the 'gate-keeper' residue of protein kinases.[26] The aminopyrazolopyrimidine group forms three specific H-bonds with main chain atoms of the hinge region (two with Val882 and one with Ala885). An additional H-bond is formed between the isoindolinone carbonyl and Lys833, which forms an additional ionic interaction with Asp836.

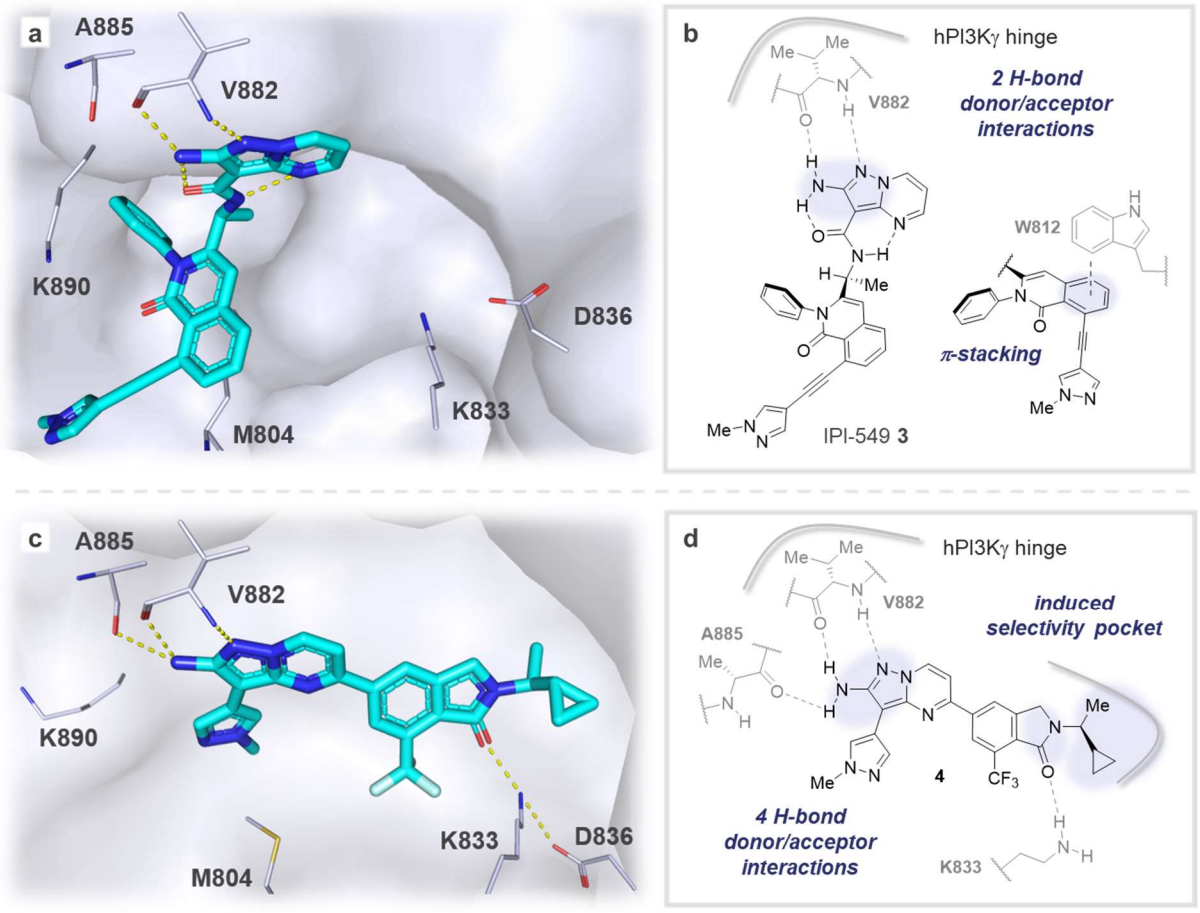

Figure 3. (a) X-Ray co-crystal structure of IPI-549 **3** bound to the active site of hPI3Kγ (PDB ID: 6XRL). H-Bonds are indicated by dashed yellow lines. (b) Schematic of the interactions of IPI-549 **3** with hPI3Kγ. (c) X-Ray co-crystal structure of **4** bound to the active site of hPI3Kγ (PDB ID: 6XRM). (d) Schematic of the interactions of lead compound **4** with hPI3Kγ.

As can be seen in **Table 1**, analog **19** that lacks a C2-amino substituent was significantly less isoform selective relative to its C2-amino congener **17**. Given that pyrazolopyrimidine **19** is limited to one hydrogen bonding interaction with Val882, this suggests that PI3Kγ selectivity is greater when the inhibitor can engage in more than one H-bonding interaction with the main chain atoms of the hinge region.

As can be seen in **Figure 4**, an overlay of the two structures shows differences in the positions of several residues. The side chain of Met804 adopts an 'up' conformation near the pyrazole group of **4** and is shifted by 4.8 Å relative to its position in the IPI-549-hPI3Kγ complex, wherein Met804 rearranges to a 'down' conformation to accommodate the quinazolinone group of the ligand (**Figure 4a**). Similarly, the

side chain of Lys833 is displaced in the **4**-hPI3Kγ complex, presumably by the C7-CF_3 group, as it participates in an H-bonding interaction with the isoindolinone carbonyl. The side chain of Lys890 is shifted by 4.9 Å and oriented away from **4** (**Figure 4b)**. Additional differences are observed in the positions and orientations of several amino acid side chains near the ligand, including Asp964 (shifted by 4.6 Å) and Tyr867.

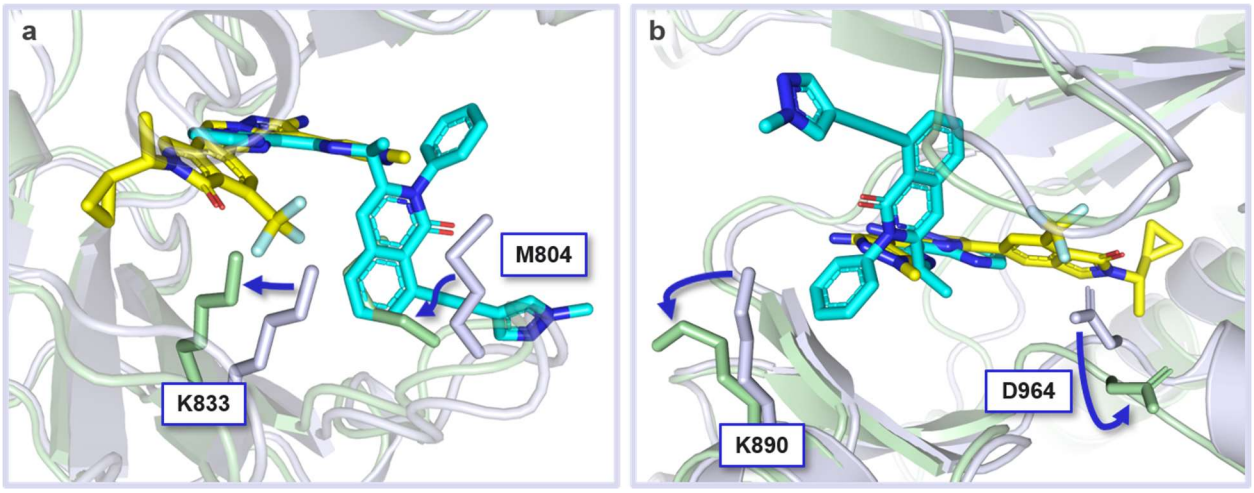

Figure 4. Alignment of co-crystal structures of hPI3Kγ complexed with IPI-549 **3** (PDB ID 6XRL; ligand colored according to the atom type, with C in cyan, N in blue and O in red; protein colored in grey) and lead **4** (PDB ID 6XRM; ligand colored according to the atom type, with C in yellow, N in blue, O in red and F in light cyan; protein colored in pale green) highlighting the different orientations observed for a) M804 and K833, and b) K890 and D964 side chains.

Synthetic Chemistry

Analogs prepared during early SAR efforts that tethered 5,6-bicyclic HBMs to the isoindolinone portion of **1** were accessed through Suzuki-Miyaura cross-coupling reactions of previously reported isoindolinone boronic ester **44**[21] and commercially available (or readily accessible) 5,6-bicyclic HBM electrophiles (e.g. **42** or **43**, **Scheme 1**).

Scheme 1. Synthesis of benzimidazole analogs (±)-**5** and (±)-**6**.[a,b]

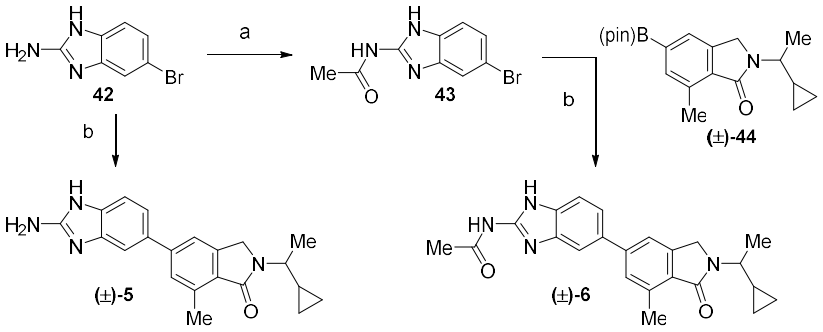

[a]Reagents and conditions: (a) AcCl, NEt_3, DCM, 14%. (b) aryl boronic acid pinacol ester (±)-**44**, $PdCl_2$(dppf), Na_2CO_3 (aq.), dioxane, 100 °C, (±)-**6** (55%), (±)-**5** (22%). [b]Aryl boronic acid pinacol ester (±)-**44** was prepared as described in the literature using racemic 1-cyclopropylethan-1-amine.[21]

In the case of triazolo-pyridines **8** and **10** (**Scheme 2**), the C2-acetamide functionality was installed after the cross-coupling via bis-acetylation followed by mono-selective transamidation with methanolic ammonia.

Scheme 2. Synthesis of PI3Kγ inhibitors bearing different hetero-bicyclic HBMs.[a,b]

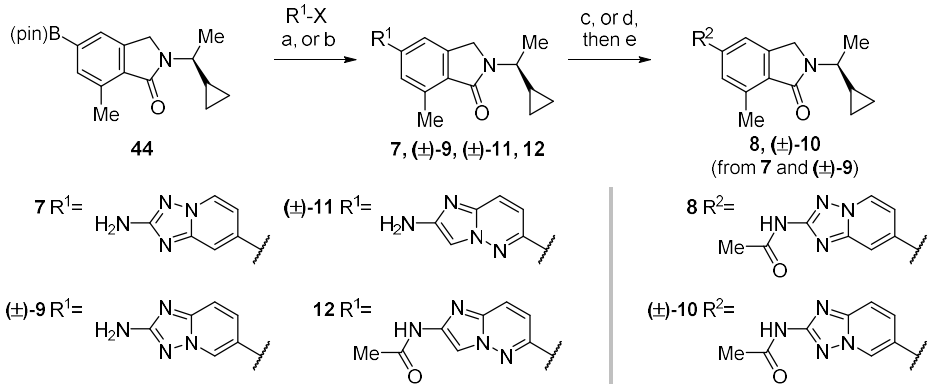

[a]Reagents and conditions: (a) *for compound* **7**, aryl halide, PCy_3 Pd G2, Na_2CO_3 (aq.), dioxane, 100 °C, 58%. (b) *for compounds* (±)-**9**, (±)-**11**, and **12**, aryl halide, $PdCl_2$(dppf), Na_2CO_3 (aq.), DME, EtOH, 100 °C. (c) *for compound* **8**, AcCl, NEt_3, CH_3CN, 0 °C to rt. (d) *for compound* **10**, Ac_2O, DIPEA, DMAP, DCM, 50 °C. (e) 7 M NH_3 in MeOH. [b]Aryl boronic acid pinacol ester **44** was prepared as described in the literature.[21]

Aryl and heteroaryl groups were generally incorporated at the 3-position of the imidazolopyridazine (e.g., **13**, **Scheme 3**) or pyrazolopyrimidine (e.g., **17**, **Scheme 5**) HBM via C3-iodination followed by cross-coupling and acidic hydrolysis of the C2-acetamide group to furnish the free

C2-amino H-bond donor. Compounds **14** and **19** (**Scheme 4**) that lack a C2-amino group were synthesized from 3-bromo-6-chloroimidazo-pyridazine **47** and 3-bromo-5-chloropyrazolopyrimidine **49**, respectively, via iterative Suzuki-Miyaura cross-coupling reactions.

Scheme 3. Synthesis of C3-substituted imidazolopyridazine **13**.[a]

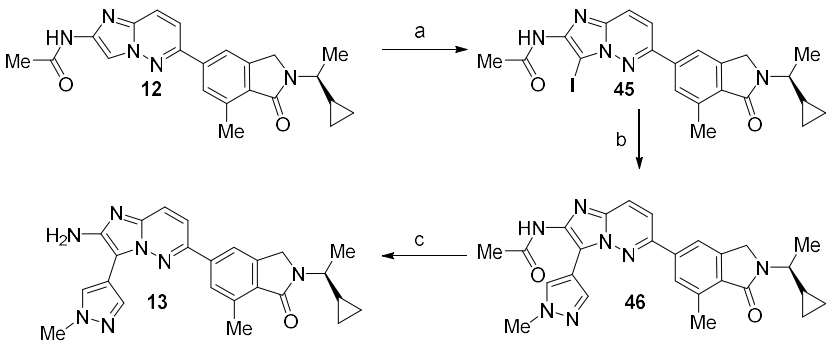

[a]Reagents and conditions: (a) NIS, $CHCl_3$, 54%. (b) 1-methyl-4-(4,4,5,5-tetramethyl-1,3,2-dioxaborolan-2-yl)-1*H*-pyrazole, $PdCl_2$(dppf), Na_2CO_3 (aq.), dioxane, 100 °C, 47%. (c) 4 M HCl in dioxane, MeOH.

Scheme 4. Synthesis of C3-substituted imidazolopyridazine and pyrazolopyrimidine analogs **14** and **19**.[a]

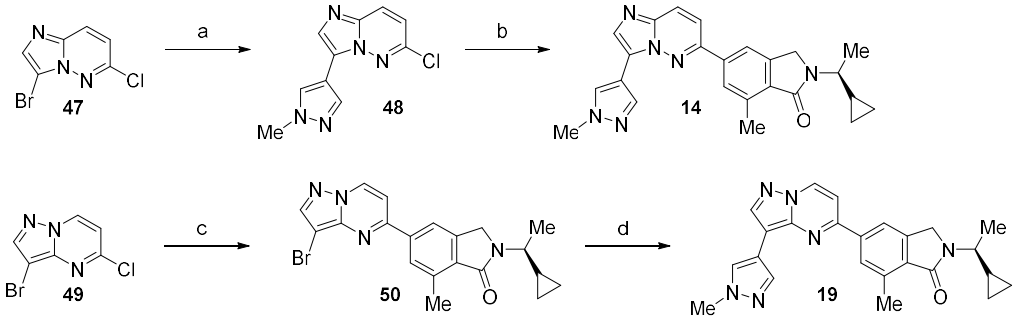

[a]Reagents and conditions: (a) 1-methyl-4-(4,4,5,5-tetramethyl-1,3,2-dioxaborolan-2-yl)-1*H*-pyrazole, $Pd(PPh_3)_4$, Na_2CO_3 (aq.), dioxane, 100 °C, 67% (b) **44**, $PdCl_2$(dppf), Na_2CO_3 (aq.), dioxane, 100 °C. (c) **44**, $PdCl_2$(dppf), Na_2CO_3 (aq.), dioxane, 80 °C, 59%. (d) 1-methyl-4-(4,4,5,5-tetramethyl-1,3,2-dioxaborolan-2-yl)-1*H*-pyrazole, $PdCl_2$(dppf), Na_2CO_3 (aq.), dioxane, 100 °C.

The first-generation synthesis of pyrazolopyrimidine **16** was blighted by a lack of published methods for the preparation of key building block 5-chloropyrazolopyrimidine **53** (**Scheme 5**). A 3-step synthesis from 1*H*-pyrazole-3,5-diamine **51** was executed, however this produced **53** in only 4% overall

yield, which hindered SAR efforts. An alternative, second-generation strategy for the preparation of C3-substituted pyrazolopyrimidine PI3Kγ inhibitors will be discussed in **Scheme 8**. Nevertheless, the synthetic route laid out in **Scheme 5** enabled a wide-range of C3-substitutents to be examined during preliminary investigations.

Scheme 5. Synthesis of pyrazolopyrimidine **16** and divergent C3-functionalization.[a]

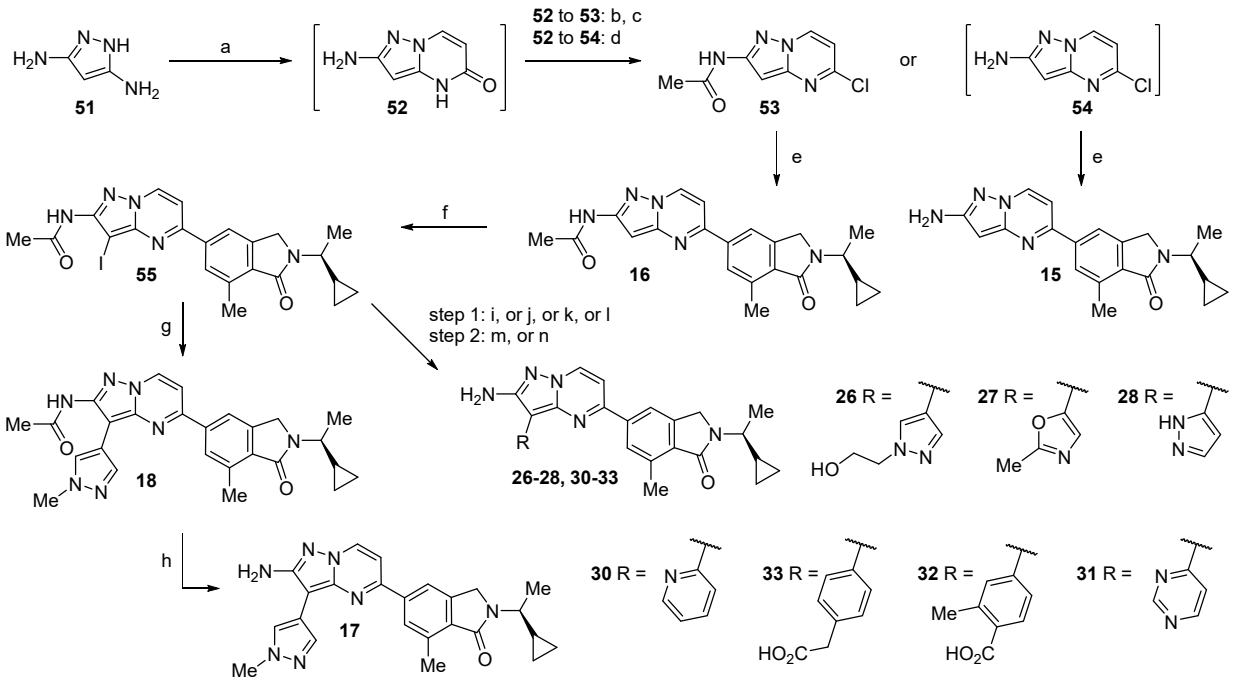

[a]Reagents and conditions: (a) 1,3-dimethyl-1,2,3,4-tetrahydropyrimidine-2,4-dione, NaOEt, EtOH, 80 °C. (b) AcCl, pyridine, CH_3CN, 0 °C to rt. (c) $POCl_3$, 80 °C, 4% from **51** over 3 steps. (d) $POCl_3$, 90 °C. (e) Aryl boronic acid pinacol ester **44**, $PdCl_2$(dppf), Na_2CO_3 (aq.), dioxane, 100 °C. (f) NIS, $CHCl_3$, 98%. (g) 1-methyl-4-(4,4,5,5-tetramethyl-1,3,2-dioxaborolan-2-yl)-1*H*-pyrazole, $PdCl_2$(dppf), Na_2CO_3 (aq.), dioxane, 90 °C. (h) 4 M HCl in dioxane, MeOH, 40 °C. (i) *for compounds* **26**, **27**, **32**, and **33**, aryl/heteroaryl boronic acid/ boronate ester, $PdCl_2$(dppf), Na_2CO_3 (aq.), dioxane, 90 °C. (j) *for compound* **30**, 2-(tributylstannyl)pyridine, Pd_2dba_3, XPhos, DMF, 135 °C. (k) *for compound* **28**, $Pd(PPh_3)_4$, 1-(oxan-2-yl)-5-(4,4,5,5-tetramethyl-1,3,2-dioxaborolan-2-yl)-1*H*-pyrazole, Na_2CO_3 (aq.), dioxane, 100 °C l) *for compound* **31**, 4-(tributylstannyl)pyrimidine, Pd_2dba_3, XPhos, DMF, 135 °C. (m) *for compounds* **26**, **27**, **28**, **30** and **31**, 4 M HCl in dioxane, MeOH, 40 °C. (n) *for compounds* **32** and **33**, 6 M NaOH (aq.), THF, MeOH, 70 °C.

In tandem to C3-modifications, the 2-position of the imidazolopyridazine was also investigated and a series of compounds (**20**-**23**) was prepared by treating 2-aminoimidazolopyridazine **11** with various acyl

chlorides in the presence of pyridine (**Scheme 6**). Similarly, mesylation of **11** gave methanesulfonamide **24**. Compound **11** could also be converted to prolinamide **25** upon reaction with triphosgene and trapping with L-prolinamide.

Scheme 6. Exploration of C2-substitution in the imidazolopyridazine series.[a]

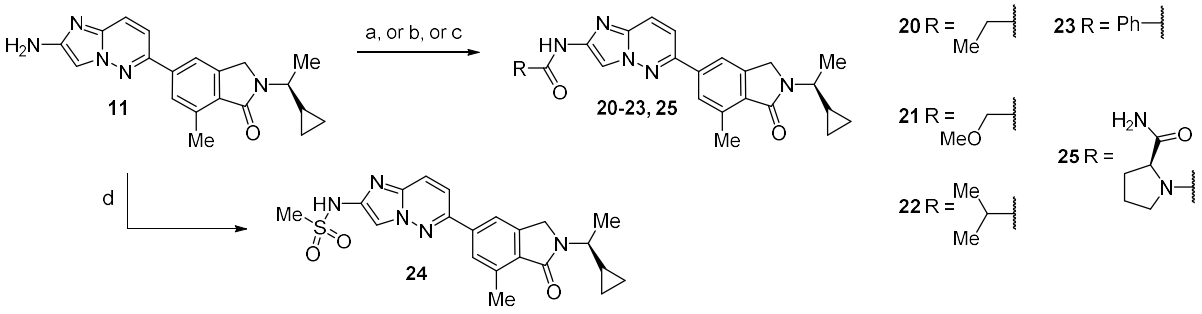

[a]Reagents and conditions: (a) *for compounds* **20**, **21**, and **22**, acyl chloride, pyridine, DCM. (b) *for compound* **23**, benzoic acid, DIPEA, HATU, DMF. (c) *for compound* **25**, L-prolinamide, DIPEA, triphosgene, DCM. (d) MsCl, NEt_3, THF.

As highlighted in **Scheme 7**, three alternative C7-isoindolinone cross-coupling partners were prepared and coupled to the pyrazolopyrimidine HBM. C7-CF_3 Isoindolinone boronic ester **58** was synthesized in 4 steps through HATU-mediated amide bond coupling between benzoic acid **56** and (*S*)-1-cyclopropylethan-1-amine, directed *ortho*-metalation of the resulting amide **57** with *sec*-BuLi and quenching with DMF, followed by deoxygenation with TFA/Et_3SiH, and borylation. Finally, Suzuki-Miyaura coupling of boronic ester **58** with 5-chloropyrazolopyrimidine **53** under standard conditions gave C7-CF_3 PI3Kγ inhibitor **34**.

The synthesis of the N-linked C7-sulfonamide building block **64** was achieved in 6 steps from methyl benzoate **59**. Radical bromination and treatment of benzyl bromide **60** with (*S*)-1-cyclopropylethan-1-amine gave C7-F isoindolinone **61**, which upon S_NAr with *para*-methoxybenzylamine and deprotection using TFA furnished C7-aniline **63**. The reaction of **63** with excess methanesulfonyl chloride, followed by TBAF-mediated selective removal of one methanesulfonyl group[29] gave C7-sulfonamide **64**. Miyaura borylation of **64** and cross-coupling with 5-chloropyrazolopyrimidine **53** gave compound **35**.

Finally, S-linked C7-sulfonamide **66** was obtained from C7-F isoindolinone **61** in 3 steps via S_NAr with benzyl mercaptan, oxidative chlorination using NCS, and coupling with methylamine hydrochloride. In this case, the final compound **36** was prepared via borylation of 5-chloropyrazolopyrimidine **53** and Suzuki-Miyaura cross-coupling with bromide **66**.

Scheme 7. Preparation of C7-modified isoindolinones and examination in pyrazolopyrimidine series.[a]

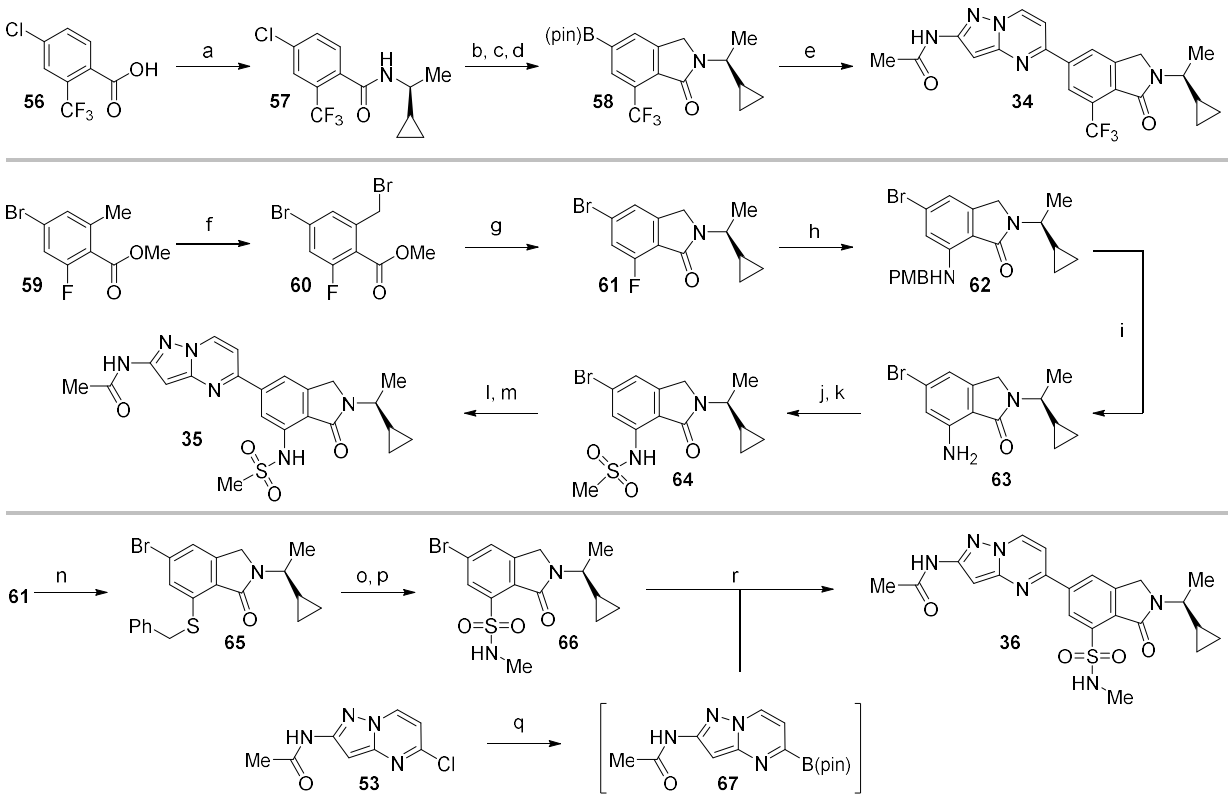

[a]Reagents and conditions: (a) (*S*)-1-cyclopropylethan-1-amine, HATU, DIPEA, DMF, 98%. (b) *sec*-BuLi (1.4 M in cyclohexane), THF, −78 °C, DMF. (c) TFA, triethylsilane, DCM, 0 °C to rt, 84% from **57** over 2 steps. (d) B_2pin_2, PCy_3 Pd G2, KOAc, dioxane, 100 °C, 68%. (e) **53**, $PdCl_2$(dppf), Na_2CO_3 (aq.), dioxane, 100 °C. (f) NBS, benzoyl peroxide (80 wt%), CCl_4, 80 °C. (g) (*S*)-1-cyclopropylethan-1-amine, $B(OH)_3$, K_2CO_3, CH_3CN, 50 °C, 58% over 2 steps from **59**. (h) $PMBNH_2$, 100 °C. (i) TFA, 40 °C, 98%. (j) MsCl, DIPEA, DMAP, DCM, 0 °C to rt. (k) TBAF, THF, 60% over 2 steps from **63**. (l) B_2pin_2, $PdCl_2$(dppf), KOAc, dioxane, 95 °C. (m) **53**, $PdCl_2$(dppf), Na_2CO_3 (aq.), dioxane, 100 °C. (n) benzyl mercaptan, K_2CO_3, DMF, 55 °C, 56%. (o) NCS, AcOH, H_2O. (p) $MeNH_2$•HCl, DIPEA, pyridine, DCM, 67% over 2 steps. (q) B_2pin_2, $PdCl_2$(dppf), KOAc, dioxane, 90 °C. (r) $PdCl_2$(dppf), Na_2CO_3 (aq.), dioxane, 100 °C, 32%.

As mentioned previously (**Scheme 5**), the first-generation approach to the pyrazolopyrimidine PI3Kγ inhibitors presented in this study relied upon a low yielding sequence for the preparation of key building block **53**. An alternative synthetic strategy to PI3Kγ inhibitors of this structural class was devised and executed that commenced from commercially available 2-bromo-5-chloropyrazolopyrimidine **68** (**Scheme 8**). Thus, selective Suzuki-Miyaura cross-coupling of **68** with isoindolinone boronic ester **58** gave intermediate **69**, which, upon Buchwald-Hartwig amination with acetamide, furnished compound **34** in just 2 steps and significantly higher overall yield. Additional C3-modifications could be evaluated in a similar fashion as described above (**Scheme 5**). This second-generation synthetic strategy will no doubt aid the discovery and characterization of additional potent and selective PI3Kγ inhibitors.

Scheme 8. Improved synthesis of pyrazolopyrimidine **34** and preparation of lead PI3Kγ inhibitor **4**.[a]

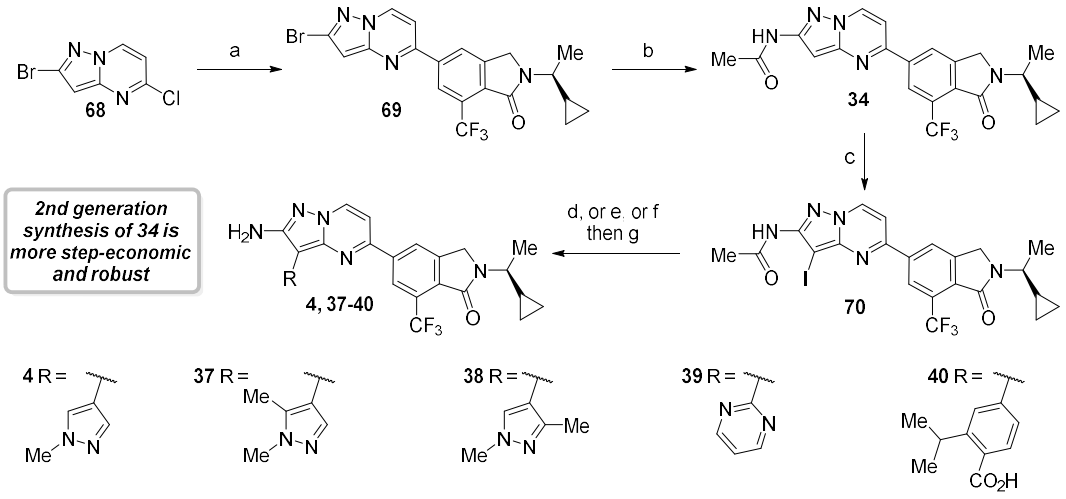

[a]Reagents and conditions: (a) boronic acid pinacol ester **58**, $PdCl_2$(dppf), Na_2CO_3 (aq.), dioxane, 80 °C, 69%. (b) acetamide, BrettPhos Pd G3, BrettPhos, Cs_2CO_3, dioxane, 100 °C, 60%. (c) NIS, CH_3CN, 88%. (d) *for compounds* **4**, **37**, and **38**, pyrazole boronic acid pinacol ester, $PdCl_2$(dppf), Na_2CO_3 (aq.), dioxane, 100 °C. (e) *for compound* **39**, 2-(tributylstannyl)pyrimidine, Pd_2dba_3, XPhos, DMF, 135 °C. (f) 2-(propan-2-yl)-4-(4,4,5,5-tetramethyl-1,3,2-dioxaborolan-2-yl)benzoic acid, $Pd(PPh_3)_4$, Na_2CO_3 (aq.), dioxane, 100 °C (g) 4 M HCl in dioxane, MeOH, 40 °C.

Conclusion

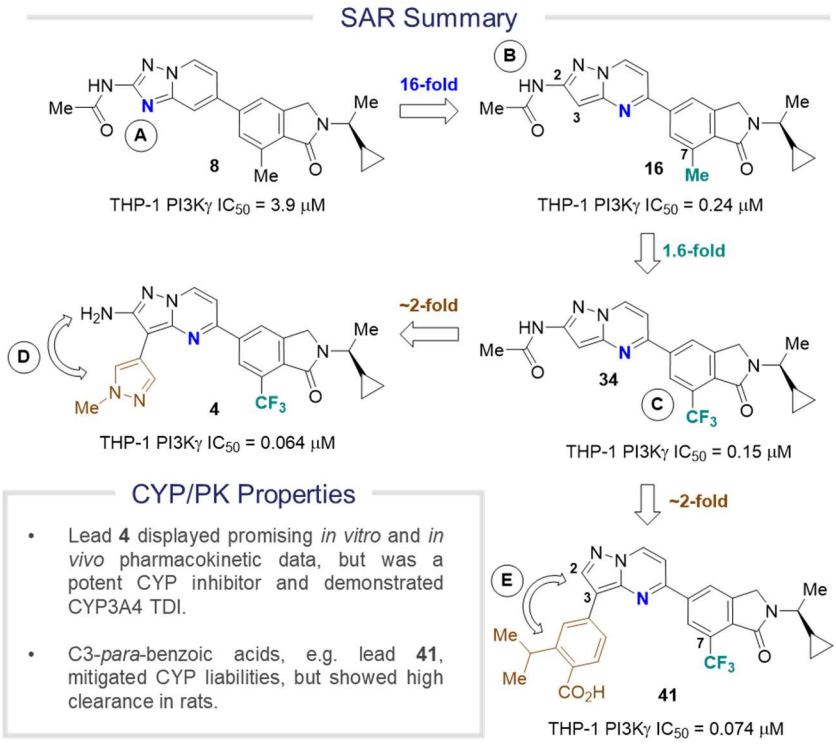

SAR	Observations
A	Positioning of N within the 5,6-heterocyclic HBM greatly impacts potency: pyrazolopyrimidine is optimal and opens C3-position for further substitution.
B	When C3 is unsubstituted the C2-amino group must be acetylated otherwise potency is lost.
C	PI3Kγ affinity can be improved by incorporating electron withdrawing/ polar substituents at C7 of the isoindolinone.
D	The C2-NH_2 group in tandem with the C3-pyrazole imparts high PI3Kγ isoform selectivity, but γ-selectivity drops if the C2-NH_2 group is replaced by –H.
E	Although C3-benzoic acids are potent, analogs are less γ-selective independent of whether C2 is substituted by –NH_2 or –H.

Figure 5. Summary of SAR findings and key trends identified during the discovery of lead PI3Kγ inhibitors **4** and **41**.

In summary, we have discovered a novel series of potent and isoform selective PI3Kγ inhibitors that feature a pyrazolopyrimidine HBM tethered to a *N*-cyclopropylethyl isoindolinone. Structural alignment of previous enzyme-bound PI3Kγ inhibitor X-ray crystal structures revealed an opportunity to target two independent mechanisms that impart γ-selectivity in class 1 PI3K inhibition, specifically 'alkyl pocket' inducement and positive interactions with the 'selectivity pocket'. This led to the early design of triazolo-pyridine **8** that demonstrated micromolar cellular potency and crucially showed no significant inhibition of the other class 1 PI3K isoforms. Additional SAR investigation, as highlighted in **Figure 5**, revealed the pyrazolopyrimidine HBM was optimal and that potency could be gained by the incorporation of electron-withdrawing groups at C7 of the isoindolinone (**8→16→34**). Incorporation of a C3-pyrazole substituent, with concurrent acetyl group removal, gave lead **4** that demonstrated a favorable PK profile in rats, but was a potent CYP3A4 inhibitor. In contrast, C3-benzoic acid incorporation and removal of the C2-acetamide group produced alternative lead **41** that was of similar potency to **4** and displayed an improved

CYP inhibition profile; however, acid **41** suffered from *supra*-hepatic clearance in rats and was less isoform selective. X-Ray crystallographic analysis of lead compound **4** bound to hPI3Kγ, as well as the SAR trends identified throughout this study, suggest that inhibitors are more selective towards PI3Kγ (relative to the other class 1 PI3K isoforms) if the hinge binding motif is able to interact through more than one hydrogen bond to the main chain atoms of the hinge region (Val882 and Ala885), when the 'alkyl pocket' is induced. Such bicyclic HBMs likely push the *N*-alkyl tail of the isoindolinone deeper into the 'alkyl pocket,' which may lead to a greater displacement of the DFG motif, resulting in improved γ-selectivity. This work will serve as a platform for future discoveries toward the optimization, development and application of PI3Kγ inhibitors for the treatment of cancer and other conditions associated with dysregulation of myeloid cell activation.

Experimental Section

General Chemistry. All reactions were performed using a Teflon-coated magnetic stir bar at the indicated temperature and were conducted under an inert atmosphere when stated. All chemicals were used as received. Reactions were monitored by TLC (silica gel 60 with fluorescence F254, visualized with a short wave/long wave UV lamp) and/or LCMS (Agilent 1100 series LCMS with UV detection at 254 nm using a binary solvent system [0.1% TFA in CH_3CN/0.1% TFA in H_2O] using either of the following columns: Agilent Eclipse Plus C18 [3.5 μm, 4.6 mm i.d. x 100 mm], Aeris Widepore C4 [3.6 μm, 2.1 mm i.d. x 50mm]). Flash chromatography was conducted on silica gel using an automated system (CombiFlash RF+ manufactured by Teledyne ISCO), with detection wavelengths of 254 and 280 nm. Reverse-phase preparative HPLC was conducted on an Agilent 1260 Infinity series HPLC. Samples were eluted using a binary solvent system (0.1% TFA in CH_3CN/0.1% TFA in H_2O) with gradient elution on a Gemini C18 110 Å column (21.2 mm i.d. x 250 mm) with detection at 254 nm. Final compounds obtained through preparative HPLC were concentrated through lyophilization. All reported yields are isolated yields. All assayed compounds were purified to ≥95% purity, as determined by LCMS (Agilent 1100 series LCMS with UV detection at 254 nm using a binary solvent system [0.1% TFA in CH_3CN/0.1% TFA in H_2O] using

either of the following columns: Agilent Eclipse Plus C18 column [3.5 μm, 4.6 mm i.d. x 100 mm], Aeris Widepore C4 column [3.6 μm, 2.1 mm i.d. x 50 mm]). LC-HRMS analysis was performed using a Shimadzu Nexera X2 UHPLC system coupled to a Q Exactive™ Hybrid Quadrupole-Orbitrap™ Mass Spectrometer. ^{1}H NMR spectra were recorded on a Varian 400 MHz NMR spectrometer equipped with an Oxford AS400 magnet or a Bruker AVII or Avance 500 MHZ NMR spectrometer. ^{13}C NMR spectra were recorded using a Bruker AVII or Avance 500 MHZ NMR spectrometer. Chemical shifts (δ) are reported as parts per million (ppm) relative to residual undeuterated solvent as an internal reference. The abbreviations s, br. s, d, t, q, dd, dt, dq, ddd, and m stand for singlet, broad singlet, doublet, triplet, quartet, doublet of doublets, doublet of triplets, doublet of quartets, doublet of doublet of doublets, and multiplet, respectively.

Compound Synthesis. ***N*-{5-[2-(1-Cyclopropylethyl)-7-methyl-1-oxo-2,3-dihydro-1*H*-isoindol-5-yl]-1*H*-1,3-benzodiazol-2-yl}acetamide** (±-**6**)**.** 5-Bromo-1*H*-1,3-benzodiazol-2-amine (205 mg, 0.97 mmol) was dissolved in DCM (4.9 mL). To this solution was added NEt_3 (0.27 mL, 1.94 mmol) followed by AcCl (0.10 mL, 1.45 mmol) and the resulting mixture was stirred for 2 h at rt. The reaction mixture was quenched with *sat. aq.* $NaHCO_3$ solution (10 mL) and diluted with DCM (40 mL) and H_2O (20 mL). The aqueous phase was separated and extracted with additional DCM (3 × 20 mL). The organic layers were combined and dried over Na_2SO_4. Concentration under reduced pressure and purification by column chromatography (SiO_2, 20% → 100% gradient of EtOAc in hexanes) produced *N*-(5-bromo-1*H*-1,3-benzodiazol-2-yl)acetamide **43** as a yellow solid (35 mg, 14% yield). ESI MS $[M+H]^+$ for $C_9H_8BrN_3O$, calcd. 254.0, found 254.0.

N-(5-Bromo-1*H*-1,3-benzodiazol-2-yl)acetamide **43** (25 mg, 0.098 mmol) and racemic isoindolinone boronate (±)-**44** (50 mg, 0.15 mmol) were dissolved in dioxane (2.0 mL). To this solution was added 1 M aq. Na_2CO_3 solution (0.4 mL) and $PdCl_2$(dppf) (23 mg, 0.020 mmol). The resulting mixture was heated at 100 °C for 1 h, then cooled to rt and diluted with EtOAc (20 mL) and H_2O (15 mL). The aqueous phase was separated and extracted with additional EtOAc (3 × 20 mL). The organic layers were combined and dried over Na_2SO_4. Concentration under reduced pressure and purification by reverse-phase HPLC furnished *N*-{5-[2-(1-cyclopropylethyl)-7-methyl-1-oxo-2,3-dihydro-1*H*-isoindol-5-yl]-1*H*-1,3-

benzodiazol-2-yl}acetamide (±)-**6** as a white solid (20 mg, 55% yield). ^{1}H NMR (400 MHz, DMSO-d_6) δ 12.00 (s, 1H), 7.79 (dd, J = 1.7, 0.7 Hz, 1H), 7.65 (s, 1H), 7.61 – 7.57 (m, 1H), 7.56 – 7.48 (m, 2H), 4.54 (s, 2H), 3.63 – 3.54 (m, 1H), 2.68 (s, 3H), 2.22 (s, 3H), 1.29 (d, J = 6.8 Hz, 3H), 1.19 – 1.08 (m, 1H), 0.64 – 0.53 (m, 1H), 0.46 – 0.33 (m, 2H), 0.29 – 0.20 (m, 1H). ESI MS $[M+H]^+$ for $C_{23}H_{24}N_4O_2$, calcd. 389.2, found 389.2.

5-(2-Amino-1*H*-1,3-benzodiazol-5-yl)-2-(1-cyclopropylethyl)-7-methyl-2,3-dihydro-1*H*-isoindol-1-one (±-**5**). The title compound was prepared in a similar manner to compound (±)-**6** from 5-bromo-1*H*-1,3-benzodiazol-2-amine **42** using racemic isoindolinone boronate (±)-**44**. ^{1}H NMR (400 MHz, DMSO-d_6) δ 12.71 (s, 1H), 8.57 (s, 2H), 7.65 (d, J = 1.5 Hz, 1H), 7.63 – 7.61 (m, 1H), 7.56 (dd, J = 8.4, 1.7 Hz, 1H), 7.52 – 7.48 (m, 1H), 7.45 (d, J = 8.3, 0.6 Hz, 1H), 4.54 (s, 2H), 3.63 – 3.54 (m, 1H), 2.68 (s, 3H), 1.29 (d, J = 6.8 Hz, 3H), 1.19 – 1.08 (m, 1H), 0.64 – 0.53 (m, 1H), 0.45 – 0.34 (m, 2H), 0.29 – 0.19 (m, 1H)..

5-{2-Amino-[1,2,4]triazolo[1,5-*a*]pyridin-7-yl}-2-[(1*S*)-1-cyclopropylethyl]-7-methyl-2,3-dihydro-1*H*-isoindol-1-one (7). 7-Bromo-[1,2,4]triazolo[1,5-*a*]pyridin-2-amine (50 mg, 0.23 mmol), isoindolinone boronate **44** (125 mg, 0.25 mmol), PCy_3 Pd G2 (7 mg, 0.012 mmol), and Na_2CO_3 (1 M aq., 0.7 mL, 0.7 mmol) were combined in dioxane (1 mL) and heated to 100 °C. Upon completion, the reaction was partitioned between EtOAc (20 mL) and H_2O (20 mL). The aqueous layer was separated and extracted with additional EtOAc (2 × 20 mL). The organic layers were combined, washed with brine (20 mL) and dried over $MgSO_4$. Concentration under reduced pressure and purification by column chromatography (SiO_2, DCM →EtOAc →DCM →10% MeOH/DCM gradient) furnished 5-{2-amino-[1,2,4]triazolo[1,5-*a*]pyridin-7-yl}-2-[(1*S*)-1-cyclopropylethyl]-7-methyl-2,3-dihydro-1*H*-isoindol-1-one **7** as a white solid (48 mg, 67%). ^{1}H NMR (400 MHz, DMSO-d_6) δ 8.63 (dd, J = 7.0, 0.8 Hz, 1H), 7.82 (s, 1H), 7.72 – 7.66 (m, 2H), 7.25 (dd, J = 7.0, 2.0 Hz, 1H), 6.09 (s, 2H), 4.54 (s, 2H), 3.64 – 3.51 (m, 1H), 2.68 (s, 3H), 1.29 (d, J = 6.8 Hz, 3H), 1.19 – 1.08 (m, 1H), 0.63 – 0.52 (m, 1H), 0.45 – 0.32 (m, 2H), 0.27 – 0.16 (m, 1H). ESI MS $[M+H]^+$ for $C_{20}H_{21}N_5O$, calcd. 348.2, found 348.2.

***N*-(7-{2-[(1*S*)-1-Cyclopropylethyl]-7-methyl-1-oxo-2,3-dihydro-1*H*-isoindol-5-yl}-[1,2,4]triazolo[1,5-*a*]pyridin-2-yl)acetamide (8)**. Compound **7** (41 mg, 0.12 mmol) and NEt_3 (70 μL, 0.47 mmol) were combined in CH_3CN (1.5 mL). The resulting mixture was cooled to 0 °C and AcCl (25 μL, 0.35 mmol) was added. The reaction was warmed to rt and stirred for 1 h. Upon completion, the reaction mixture was filtered, rinsing with DCM. Concentration under reduced pressure furnished a mixture of mono and bis-acetylated material that was taken on crude to the next step. To the crude material from the previous step was added excess 7 N NH_3 in MeOH (0.4 mL) and the reaction was stirred for 30 min. The solution was concentrated and purified by reverse-phase HPLC to yield *N*-(7-{2-[(1*S*)-1-cyclopropylethyl]-7-methyl-1-oxo-2,3-dihydro-1*H*-isoindol-5-yl}-[1,2,4]triazolo[1,5-*a*]pyridin-2-yl)acetamide **8**. ^{1}H NMR (400 MHz, DMSO-d_6) δ 10.83 (s, 1H), 8.93 (dd, J = 7.1, 0.8 Hz, 1H), 8.02 (dd, J = 2.0, 0.9 Hz, 1H), 7.87 (s, 1H), 7.73 (s, 1H), 7.49 (dd, J = 7.1, 2.0 Hz, 1H), 4.54 (s, 2H), 3.64 – 3.50 (m, 1H), 2.68 (s, 3H), 2.20 (s, 3H), 1.28 (d, J = 6.8 Hz, 3H), 1.18 – 1.07 (m, 1H), 0.60 – 0.51 (m, 1H), 0.45 – 0.31 (m, 2H), 0.28 – 0.15 (m, 1H). ESI MS $[M+H]^+$ for $C_{22}H_{23}N_5O_2$, calcd. 390.2, found 390.2.

5-{2-Aminoimidazo[1,2-*b*]pyridazin-6-yl}-2-(1-cyclopropylethyl)-7-methyl-2,3-dihydro-1*H*-isoindol-1-one (±-**11**). To a reaction vessel containing isoindolinone boronate (±)-**44** (150 mg, 0.44 mmol) was added 6-chloroimidazo[1,2-*b*]pyridazine-2-amine (57 mg, 0.34 mmol), $PdCl_2$(dppf) (12 mg, 0.017 mmol) and Na_2CO_3 (53.7 mg, 0.51 mmol). A solution of DME, H_2O, and EtOH (7:3:2 ratio, 2.3 ml, 0.15 M) was added. The reaction was sealed and heated to 90 °C for 4 h. Upon reaction completion by LC/MS, the mixture was cooled to rt, filtered through celite and concentrated under reduced pressure. The resulting residue was purified by column chromatography (SiO_2, 50% →100% EtOAc/hexane, followed by 10% MeOH/DCM), then reverse-phase HPLC, which afforded the desired 5-{2-aminoimidazo[1,2-*b*]pyridazin-6-yl}-2-(1-cyclopropylethyl)-7-methyl-2,3-dihydro-1*H*-isoindol-1-one (±)-**11**. ^{1}H NMR (400 MHz, DMSO-d_6) δ 8.02 (s, 1H), 7.96 (d, J = 9.3 Hz, 1H), 7.88 (s, 1H), 7.83 (d, J = 9.3 Hz, 1H), 7.53 (s, 1H), 4.55 (s, 2H), 3.56 (dq, J = 9.3, 6.8 Hz, 1H), 2.68 (s, 3H), 1.28 (d, J = 6.8 Hz, 3H), 1.18 – 1.05 (m, 1H), 0.61 – 0.53 (m, 1H), 0.45 – 0.30 (m, 2H), 0.26 – 0.17 (m, 1H). ESI MS $[M+H]^+$ for $C_{20}H_{21}N_5O$, calcd. 348.2, found 348.2

5-{2-Amino-[1,2,4]triazolo[1,5-*a*]pyridin-6-yl}-2-(1-cyclopropylethyl)-7-methyl-2,3-dihydro-1*H*-isoindol-1-one (±-**9**). The title compound was prepared in a similar manner to compound (±)-**11** using 6-bromo[1,2,4]triazolo[1,5-*a*]pyridin-2-amine as the electrophile. ^{1}H NMR (400 MHz, DMSO-d_6) δ 9.03 (s, 1H), 7.92 (d, J = 9.2 Hz, 1H), 7.75 (s, 1H), 7.62 (s, 1H), 7.52 (d, J = 9.2 Hz, 1H), 4.51 (s, 2H), 3.55 (dq, J = 9.3, 7.0 Hz, 1H), 2.64 (s, 3H), 1.27 (d, J = 7.0 Hz, 3H), 1.15 – 1.09 (m, 1H), 0.58 – 0.53 (m, 1H), 0.41 – 0.34 (m, 2H), 0.23 – 0.19 (m, 1H). ESI MS $[M+H]^+$ for $C_{20}H_{21}N_5O$, calcd. 348.2, found 348.2.

***N*-{6-[2-(1-Cyclopropylethyl)-7-methyl-1-oxo-2,3-dihydro-1*H*-isoindol-5-yl]-[1,2,4]triazolo[1,5-*a*]pyridin-2-yl}acetamide** (±-**10**). To a solution of compound (±)-**9** (67 mg, 0.19 mmol), diisopropylethylamine (0.13 mL, 0.77 mmol), and DMAP (2.4 mg, 0.019 mmol) in THF (1.0 mL, 0.2 M) was added acetic anhydride (55 µl, 0.579 mmol). The resulting solution was heated to 50 °C for 3 h, at which point additional diisopropylethylamine (0.13 mL, 0.77 mmol) and acetic anhydride (55 µl, 0.579 mmol) were added, and the reaction was heated for an additional 16 h. The resulting solution was concentrated in vacuo and purified by column chromatography (SiO_2, 0→10% MeOH/DCM) to provide bis-acylated material as the major product. This crude material was taken up in 1 ml of 7 N NH_3 in MeOH and stirred at rt for 2 h. Upon completion, the reaction was concentrated and purified by reverse phase HPLC to yield the desired product *N*-{6-[2-(1-cyclopropylethyl)-7-methyl-1-oxo-2,3-dihydro-1*H*-isoindol-5-yl]-[1,2,4]triazolo[1,5-*a*]pyridin-2-yl}acetamide (±)-**10**. ^{1}H NMR (400 MHz, DMSO-d_6) δ 10.85 (s, 1H), 9.28 (s, 1H), 8.02 (d, J = 9.3 Hz, 1H), 7.80 (s, 1H), 7.77 (d, J = 9.3 Hz, 1H), 7.67 (s, 1H), 4.52 (s, 2H), 3.56 (dq, J = 9.4, 6.8 Hz, 1H), 2.66 (s, 3H), 2.14 (br. s, 3H), 1.27 (d, J = 6.8 Hz, 3H), 1.17 – 1.09 (m, 1H), 0.59 – 0.53 (m, 1H), 0.42 – 0.33 (m, 2H), 0.24 – 0.17 (m, 1H). ESI MS $[M+H]^+$ for $C_{22}H_{23}N_5O_2$, calcd. 390.2, found 390.0.

***N*-(6-{2-[(1*S*)-1-Cyclopropylethyl]-7-methyl-1-oxo-2,3-dihydro-1*H*-isoindol-5-yl}imidazo[1,2-*b*]pyridazin-2-yl)acetamide (12)**. The title compound was prepared in a similar manner to compound (±)-**11** using *N*-(6-chloroimidazo[1,2-*b*]pyridazin-2-yl)acetamide as the electrophile. ^{1}H NMR (400 MHz, DMSO-d_6) δ 10.93 (s, 1H), 8.30 (s, 1H), 8.09 (d, J = 9.5 Hz, 1H), 8.05 (s, 1H), 7.91 (s, 1H), 7.82 (s, J = 9.5 Hz, 1H), 4.56 (s, 2H), 3.56 (dq, J = 8.7, 6.7 Hz, 1H), 2.69 (s, 3H), 2.10 (s, 3H), 1.28 (d, J =

6.7 Hz, 3H), 1.17 – 1.08 (m, 1H), 0.58 – 0.53 (m, 1H), 0.43 – 0.34 (m, 2H), 0.26 – 0.19 (m, 1H). ESI MS $[M+H]^+$ for $C_{22}H_{23}N_5O_2$, calcd. 390.2, found 390.2.

5-[2-Amino-3-(1-methyl-1*H*-pyrazol-4-yl)imidazo[1,2-*b*]pyridazin-6-yl]-2-[(1*S*)-1-cyclopropylethyl]-7-methyl-2,3-dihydro-1*H*-isoindol-1-one (13). To a solution of compound **12** (150 mg, 0.39 mmol) in $CHCl_3$ (7.7 ml) was added NIS (173 mg, 0.77 mmol). The reaction was wrapped in foil to exclude light and was stirred at rt for 35 min. Upon completion, the reaction was concentrated onto celite and purified by column chromatography (SiO_2, 0→10% MeOH in DCM) to yield the iodinated product **45** (107 mg, 54% yield). ESI MS $[M+H]^+$ for $C_{22}H_{22}IN_5O_2$, calcd. 516.1, found 516.0.

The iodinated product **45** (100 mg, 0.194 mmol) was combined with 1-methyl-4-(4,4,5,5-tetramethyl-1,3,2-dioxaborolan-2-yl)-1*H*-pyrazole (81 mg, 0.39 mmol), Pd(dppf)Cl_2 (14 mg, 0.02 mmol) and 2.0 M aq. Na_2CO_3 (0.28 mL, 0.56 mmol) in dioxane (1.9 mL) and heated to 100 °C. After 4 h, additional boronic ester (81 mg, 0.39 mmol) and Pd(dppf)Cl_2 (14 mg, 0.02 mmol) were added, and the reaction was stirred for an additional 2 h at 100 °C. The resulting mixture was filtered through celite and concentrated under reduced pressure. Purification by column chromatography (SiO_2, 0→7% MeOH/DCM) afforded the cross-coupled product **46** (43 mg, 47% yield) that was used directly in the next step. ESI MS $[M+H]^+$ for $C_{26}H_{27}N_7O_2$, calcd. 428.2, found 428.2.

The product acetamide was taken up in MeOH (0.9 mL) and 4 N HCl in dioxane (0.29 mL) was added. The reaction was stirred for 24 h, and upon completion, was concentrated and purified by reverse-phase HPLC to yield the desired 5-[2-amino-3-(1-methyl-1*H*-pyrazol-4-yl)imidazo[1,2-*b*]pyridazin-6-yl]-2-[(1*S*)-1-cyclopropylethyl]-7-methyl-2,3-dihydro-1*H*-isoindol-1-one **13**. ^{1}H NMR (400 MHz, DMSO-d_6) δ 8.49 (s, 1H), 8.29 (s, 1H), 8.11 (s, 1H), 7.92 (s, 1H), 7.89 (d, J = 9.2 Hz, 1H), 7.71 (d, J = 9.2 Hz, 1H), 4.60 (s, 2H), 3.97 (s, 3H), 3.58 (dq, J = 9.3, 6.8 Hz, 1H), 2.72 (s, 3H), 1.29 (d, J = 6.8 Hz, 3H), 1.15 – 1.13 (m, 1H), 0.58 – 0.55 (m, 1H), 0.42 – 0.36 (m, 2H), 0.25 – 0.22 (m, 1H). ESI MS $[M+H]^+$ for $C_{24}H_{25}N_7O$, calcd. 428.2, found 428.2

2-[(1*S*)-1-Cyclopropylethyl]-7-methyl-5-[3-(1-methyl-1*H*-pyrazol-4-yl)imidazo[1,2-*b*]pyridazin-6-yl]-2,3-dihydro-1*H*-isoindol-1-one (14). A solution of 3-bromo-6-chloroimidazo[1,2-

b]pyridazine **47** (200 mg, 0.86 mmol), 1-methyl-4-(4,4,5,5-tetramethyl-1,3,2-dioxaborolan-2-yl)-1*H*-pyrazole (197 mg, 0.95 mmol), $Pd(PPh_3)_4$ (99.4 mg, 0.086 mmol), and 2.0 M aq. Na_2CO_3 (1.3 mL) in dioxane (8.6 mL) was heated to 100 °C overnight. Upon completion, the reaction was filtered through celite. Concentration under reduced pressure and purification by column chromatography (SiO_2, 0→100% EtOAc in hexanes) yielded the aryl chloride intermediate **48** (138 mg, 67% yield). ESI MS $[M+H]^+$ for $C_{10}H_8ClN_5$, calcd. 234.0, found 234.1.

The product chloride **48** (50 mg, 0.214 mmol, 1 equiv) was combined with isoindolinone boronate **44** (110 mg, 0.32 mmol), $Pd(dppf)Cl_2$ (16 mg, 0.020 mmol) and 2.0 M aq. Na_2CO_3 (0.32 mL) in dioxane (2.1 mL) and the resulting solution was heated to 100 °C overnight. The reaction was concentrated in vacuo and purified by reverse-phase HPLC to yield the desired product 2-[(1*S*)-1-cyclopropylethyl]-7-methyl-5-[3-(1-methyl-1*H*-pyrazol-4-yl)imidazo[1,2-*b*]pyridazin-6-yl]-2,3-dihydro-1*H*-isoindol-1-one **14**. ^{1}H NMR (400 MHz, DMSO-d_6) δ 8.53 (s, 1H), 8.36 (d, J = 9.5 Hz, 1H), 8.24 (d, J = 9.2 Hz, 2H), 8.19 (s, 1H), 8.00 – 7.96 (m, 2H), 4.62 (s, 2H), 3.98 (s, 3H), 3.58 (dq, J = 9.2, 6.8 Hz, 1H), 2.73 (s, 3H), 1.29 (d, J = 6.8 Hz, 3H), 1.19 – 1.10 (m, 1H), 0.60 – 0.55 (m, 1H), 0.44 – 0.35 (m, 2H), 0.26 – 0.22 (m, 1H). ESI MS $[M+H]^+$ for $C_{24}H_{24}N_6O$, calcd. 413.2, found 413.1.

2-[(1*S*)-1-Cyclopropylethyl]-7-methyl-5-[3-(1-methyl-1*H*-pyrazol-4-yl)pyrazolo[1,5-*a*]pyrimidin-5-yl]-2,3-dihydro-1*H*-isoindol-1-one (19). The title compound was prepared in a similar fashion to compound **14** using 3-bromo-5-chloropyrazolo[1,5-*a*]pyrimidine **49** as the starting material and iterative cross-couplings with isoindolinone boronate **44**, followed by 1-methyl-4-(4,4,5,5-tetramethyl-1,3,2-dioxaborolan-2-yl)-1*H*-pyrazole. ^{1}H NMR (400 MHz, DMSO-d_6) δ 9.19 (d, J = 7.4 Hz, 1H), 8.53 (s, 1H), 8.39 – 8.35 (m, 1H), 8.29 (s, 1H), 8.19 – 8.14 (m, 1H), 8.08 (d, J = 0.8 Hz, 1H), 7.71 (d, J = 7.5 Hz, 1H), 4.63 (s, 2H), 3.95 (s, 3H), 3.66 – 3.56 (m, 1H), 2.75 (s, 3H), 1.31 (d, J = 6.8 Hz, 3H), 1.21 – 1.11 (m, 1H), 0.66 – 0.54 (m, 1H), 0.49 – 0.34 (m, 2H), 0.30 – 0.20 (m, 1H). ESI MS $[M+H]^+$ for $C_{24}H_{24}N_6O$, calcd. 413.2, found 413.2.

***N*-(5-{2-[(1*S*)-1-Cyclopropylethyl]-7-methyl-1-oxo-2,3-dihydro-1*H*-isoindol-5-yl}pyrazolo[1,5-*a*]pyrimidin-2-yl)acetamide (16)**. A flask was charged with 1*H*-pyrazole-3,5-diamine **51**

(2.50 g, 25.5 mmol), 1,3-dimethyl-1,2,3,4-tetrahydropyrimidine-2,4-dione (3.60 g, 25.5 mmol), and EtOH (70 mL). NaOEt (21 wt.% in EtOH, 8 mL) was added and the resulting mixture was heated to 80 °C and stirred for 15 h. The reaction mixture was cooled to rt and the solid crude product **52** was isolated by filtration, dried under reduced pressure, and taken immediately onto the next step (2.23 g crude mass). ESI MS $[M+H]^+$ for $C_6H_6N_4O$, calcd. 151.1, found 151.1.

Crude 2-amino-4*H*,5*H*-pyrazolo[1,5-*a*]pyrimidin-5-one **52** (2.23 g) was dissolved in pyridine (7.2 mL) and CH_3CN (60 mL). The resulting mixture was cooled to 0 °C and AcCl (5.3 mL, 74 mmol) was added, and the reaction was warmed to rt. After 40 min, the reaction was quenched with *sat. aq.* $NaHCO_3$ solution (100 mL) and diluted with EtOAc (100 mL). The aqueous phase was separated and back extracted with additional EtOAc (2 × 75 mL). The organic layers were combined, dried over $MgSO_4$, and concentrated under reduced pressure with azeotropic removal of pyridine using toluene, which afforded crude bis-acetylated product that was taken directly onto the next step without purification (660 mg). The crude product (660 mg) from the previous step was cautiously added to $POCl_3$ (4 mL) at 0 °C. The resulting mixture was heated to 80 °C and stirred for 30 min. The reaction was carefully poured onto ice and quenched by the slow addition of K_2CO_3 (excess), with stirring, and diluted with DCM (100 mL). The aqueous layer was separated and back extracted with additional DCM (2 × 75 mL). The organic layers were combined, washed with H_2O (100 mL), brine (100 mL) and dried over $MgSO_4$. Concentration under reduced pressure furnished *N*-{5-chloropyrazolo[1,5-*a*]pyrimidin-2-yl}acetamide **53** (225 mg, 1.1 mmol, 4% from **51** over 3 steps) that was of sufficient purity to use in subsequent steps. ESI MS $[M+H]^+$ for $C_8H_7ClN_4O$, calcd. 211.0, found 211.1.

The final compound *N*-(5-{2-[(1*S*)-1-Cyclopropylethyl]-7-methyl-1-oxo-2,3-dihydro-1*H*-isoindol-5-yl}pyrazolo[1,5-*a*]pyrimidin-2-yl)acetamide **16** was prepared in a similar fashion to compound (±)-**6** using *N*-{5-chloropyrazolo[1,5-a]pyrimidin-2-yl}acetamide **53** and isoindolinone boronate **44**. ^{1}H NMR (400 MHz, DMSO-d_6) δ 10.96 (s, 1H), 9.08 (dd, J = 7.3, 0.9 Hz, 1H), 8.22 (s, 1H), 8.07 (s, 1H), 7.63 (d, J = 7.4 Hz, 1H), 6.94 (s, 1H), 4.58 (s, 2H), 3.63 – 3.54 (m, 1H), 2.71 (s, 3H), 2.12 (s, 3H), 1.30 (d, J = 6.8

Hz, 3H), 1.22 – 1.08 (m, 1H), 0.64 – 0.54 (m, 1H), 0.48 – 0.34 (m, 2H), 0.28 – 0.20 (m, 1H). ESI MS $[M+H]^+$ for $C_{22}H_{23}N_5O_2$, calcd. 390.2, found 390.2.

5-{2-Aminopyrazolo[1,5-*a*]pyrimidin-5-yl}-2-[(1*S*)-1-cyclopropylethyl]-7-methyl-2,3-dihydro-1*H*-isoindol-1-one (15). The title compound was prepared in a similar fashion to compound **16**; however, the acetylation step was omitted, and crude 2-amino-4*H*,5*H*-pyrazolo[1,5-*a*]pyrimidin-5-one **52** was treated directly with $POCl_3$, and the resulting 5-chloropyrazolo[1,5-*a*]pyrimidin-2-amine **54** (crude) cross-coupled with isoindolinone boronate **44**, as described for compound **16**. ^{1}H NMR (400 MHz, chloroform-*d*) δ 8.43 (dd, *J* = 7.2, 0.8 Hz, 1H), 7.96 (s, 1H), 7.84 (s, 1H), 7.08 (d, *J* = 7.2 Hz, 1H), 5.99 (d, *J* = 0.8 Hz, 1H), 4.61 – 4.40 (m, 2H), 3.78 (dt, *J* = 9.4, 6.8 Hz, 1H), 2.81 (s, 3H), 1.36 (d, *J* = 6.8 Hz, 3H), 1.11 – 0.98 (m, 1H), 0.70 – 0.58 (m, 1H), 0.51 – 0.32 (m, 3H). ESI MS $[M+H]^+$ for $C_{20}H_{21}N_5O$, calcd. 348.2, found 348.2.

***N*-(5-{2-[(1*S*)-1-Cyclopropylethyl]-7-methyl-1-oxo-2,3-dihydro-1*H*-isoindol-5-yl}-3-(1-methyl-1*H*-pyrazol-4-yl)pyrazolo[1,5-*a*]pyrimidin-2-yl)acetamide (18)**. *N*-(5-{2-[(1*S*)-1-Cyclopropylethyl]-7-methyl-1-oxo-2,3-dihydro-1*H*-isoindol-5-yl}-3-iodopyrazolo[1,5-*a*]pyrimidin-2-yl)acetamide **55** was prepared in a similar fashion to iodide **45** from compound **16** (195 mg, 98%). ESI MS $[M+H]^+$ for $C_{22}H_{22}IN_5O_2$, calcd. 516.1, found 516.0. The title compound was accessed in analogous fashion to compound **46** via cross-coupling of iodide **55** with 1-methyl-4-(4,4,5,5-tetramethyl-1,3,2-dioxaborolan-2-yl)-1*H*-pyrazole. ^{1}H NMR (400 MHz, DMSO-d_6) δ 10.17 (s, 1H), 9.13 (d, *J* = 7.4 Hz, 1H), 8.35 (s, 1H), 8.15 (s, 1H), 8.10 (s, 1H), 7.99 (s, 1H), 7.74 (d, *J* = 7.4 Hz, 1H), 4.63 (s, 2H), 3.95 (s, 3H), 3.68 – 3.50 (m, 1H), 2.75 (s, 3H), 2.10 (s, 3H), 1.31 (d, *J* = 6.9 Hz, 3H), 1.22 – 1.09 (m, 1H), 0.63 – 0.54 (m, 1H), 0.48 – 0.36 (m, 2H), 0.30 – 0.20 (m, 1H). ESI MS $[M+H]^+$ for $C_{26}H_{27}N_7O_2$, calcd. 470.2, found 470.2.

5-[2-Amino-3-(1-methyl-1*H*-pyrazol-4-yl)pyrazolo[1,5-*a*]pyrimidin-5-yl]-2-[(1*S*)-1-cyclopropylethyl]-7-methyl-2,3-dihydro-1*H*-isoindol-1-one (17). The title compound was prepared in a similar fashion to compound **13** from *N*-(5-{2-[(1*S*)-1-cyclopropylethyl]-7-methyl-1-oxo-2,3-dihydro-1*H*-isoindol-5-yl}-3-(1-methyl-1*H*-pyrazol-4-yl)pyrazolo[1,5-*a*]pyrimidin-2-yl)acetamide **18**. ^{1}H NMR (400

MHz, DMSO-d_6) δ 8.81 (d, J = 7.2 Hz, 1H), 8.27 (s, 1H), 8.23 (s, 1H), 8.13 (d, J = 0.8 Hz, 1H), 8.07 (s, 1H), 7.38 (d, J = 7.2 Hz, 1H), 4.61 (s, 2H), 3.93 (s, 3H), 3.65 – 3.54 (m, 1H), 2.73 (s, 3H), 1.30 (d, J = 6.8 Hz, 3H), 1.21 – 1.10 (m, 1H), 0.65 – 0.54 (m, 1H), 0.47 – 0.34 (m, 2H), 0.31 – 0.20 (m, 1H). ^{13}C NMR (125 MHz, DMSO-d_6) δ 167.0, 157.7, 152.9, 144.5, 143.0, 139.2, 136.4, 136.0, 134.4, 130.9, 128.2, 126.7, 119.2, 112.1, 102.1, 86.8, 51.4, 45.4, 38.6, 18.1, 16.9, 15.6, 3.9, 3.3. ESI HRMS $[M+H]^+$ for $C_{24}H_{25}N_7O$, calcd. 428.2193, found 428.2191.

***N*-(6-{2-[(1*S*)-1-Cyclopropylethyl]-7-methyl-1-oxo-2,3-dihydro-1*H*-isoindol-5-yl}imidazo[1,2-*b*]pyridazin-2-yl)propenamide (20)**. To a solution of 5-{2-aminoimidazo[1,2-*b*]pyridazin-6-yl}-2-[(1*S*)-1-cyclopropylethyl]-7-methyl-2,3-dihydro-1*H*-isoindol-1-one **11** (30 mg, 0.086 mmol) in DCM (0.43 mL) and pyridine (35 μL, 0.43 mmol) was added propionyl chloride (23 μL, 0.26 mmol). The reaction was complete within 1 h, concentrated, and purified by reverse-phase HPLC to yield the desired compound *N*-(6-{2-[(1*S*)-1-cyclopropylethyl]-7-methyl-1-oxo-2,3-dihydro-1*H*-isoindol-5-yl}imidazo[1,2-*b*]pyridazin-2-yl)propenamide **20**. ^{1}H NMR (400 MHz, DMSO-d_6) δ 10.89 (s, 1H), 8.32 (s, 1H), 8.09 (d, J = 9.5 Hz, 1H), 8.05 (s, 1H), 7.91 (s, 1H), 7.82 (d, J = 9.5 Hz, 1H), 4.56 (s, 2H), 3.63 – 3.55 (m, 1H), 2.69 (s, 3H), 2.40 (q, J = 7.5 Hz, 2H), 1.28 (d, J = 7.5 Hz, 3H), 1.17 – 1.07 (m, 4H), 0.59 – 0.53 (m, 1H), 0.43 – 0.34 (m, 2H), 0.25 – 0.20 (m, 1H). ESI MS $[M+H]^+$ for $C_{23}H_{25}N_5O_2$, calcd. 404.2, found 404.2.

***N*-(6-{2-[(1*S*)-1-Cyclopropylethyl]-7-methyl-1-oxo-2,3-dihydro-1*H*-isoindol-5-yl}imidazo[1,2-*b*]pyridazin-2-yl)-2-methoxyacetamide (21)**. The title compound was prepared in a similar manner to compound **20** using methoxyacetyl chloride. ^{1}H NMR (400 MHz, DMSO-d_6) δ 10.76 (s, 1H), 8.37 (d, J = 0.7 Hz, 1H), 8.17 – 8.04 (m, 2H), 7.93 (dd, J = 1.6, 0.9 Hz, 1H), 7.86 (d, J = 9.5 Hz, 1H), 4.58 (s, 2H), 4.11 (s, 2H), 3.65 – 3.52 (m, 1H), 3.38 (s, 3H), 2.71 (s, 3H), 1.30 (d, J = 6.8 Hz, 3H), 1.20 – 1.09 (m, 1H), 0.65 – 0.53 (m, 1H), 0.47 – 0.33 (m, 2H), 0.29 – 0.19 (m, 1H). ESI MS $[M+H]^+$ for $C_{23}H_{25}N_5O_3$, calcd 420.2, found 420.2.

***N*-(6-{2-[(1*S*)-1-Cyclopropylethyl]-7-methyl-1-oxo-2,3-dihydro-1*H*-isoindol-5-yl}imidazo[1,2-*b*]pyridazin-2-yl)-2-methylpropanamide (22)**. The title compound was prepared in a

similar manner to compound **20** using isobutyryl chloride. ^{1}H NMR (400 MHz, DMSO-d_6) δ 10.90 (s, 1H), 8.34 (s, 1H), 8.14 – 8.04 (m, 2H), 7.92 (dd, J = 1.6, 0.9 Hz, 1H), 7.84 (d, J = 9.5 Hz, 1H), 4.58 (s, 2H), 3.64 – 3.52 (m, 1H), 2.81 – 2.70 (m, 1H), 2.71 (s, 3H), 1.29 (d, J = 6.8 Hz, 3H), 1.19 – 1.11 (m, 1H), 1.12 (d, J = 6.8 Hz, 6H), 0.63 – 0.52 (m, 1H), 0.40 (ddp, J = 14.4, 9.4, 5.2 Hz, 2H), 0.29 – 0.19 (m, 1H). ESI MS $[M+H]^+$ for $C_{24}H_{27}N_5O_2$, calcd. 418.2, found 418.2.

***N*-(6-{2-[(1*S*)-1-Cyclopropylethyl]-7-methyl-1-oxo-2,3-dihydro-1*H*-isoindol-5-yl}imidazo[1,2-*b*]pyridazin-2-yl)benzamide (23)**. To a solution of 5-{2-aminoimidazo[1,2-*b*]pyridazin-6-yl}-2-[(1*S*)-1-cyclopropylethyl]-7-methyl-2,3-dihydro-1*H*-isoindol-1-one **11** (30 mg, 0.086 mmol) and benzoic acid (21 mg, 0.172 mmol) in DMF (0.9 mL) was added diisopropylethylamine (60 µL, 0.344 mmol) followed by HATU (65 mg, 0.172 mmol). The reaction was monitored by LCMS, and upon completion was filtered and purified by reverse-phase HPLC to yield the title compound **23**. ^{1}H NMR (400 MHz, DMSO-d_6) δ 11.48 (s, 1H), 8.56 (d, J = 0.6 Hz, 1H), 8.17 (dd, J = 9.5, 0.7 Hz, 1H), 8.14 – 8.07 (m, 3H), 7.96 (s, 1H), 7.89 (d, J = 9.5 Hz, 1H), 7.66 – 7.57 (m, 1H), 7.59 – 7.49 (m, 2H), 4.59 (s, 2H), 3.65 – 3.53 (m, 1H), 2.72 (s, 3H), 1.30 (d, J = 6.8 Hz, 3H), 1.22 – 1.09 (m, 1H), 0.64 – 0.53 (m, 1H), 0.48 – 0.34 (m, 2H), 0.30 – 0.20 (m, 1H). ESI MS $[M+H]^+$ for $C_{27}H_{25}N_5O_2$, calcd. 452.2, found 452.2.

***N*-(6-{2-[(1*S*)-1-Cyclopropylethyl]-7-methyl-1-oxo-2,3-dihydro-1*H*-isoindol-5-yl}imidazo[1,2-*b*]pyridazin-2-yl)methanesulfonamide (24)**. To a solution of 5-{2-aminoimidazo[1,2-*b*]pyridazin-6-yl}-2-[(1*S*)-1-cyclopropylethyl]-7-methyl-2,3-dihydro-1*H*-isoindol-1-one **11** (30 mg, 0.090 mmol) in THF (1.2 ml) was added triethylamine (18 µL, 0.13 mmol) followed by MsCl (8 µL, 0.103 mmol). The reaction was stirred at rt for 2 h and quenched by partitioning between EtOAc and *sat*. *aq*. NH_4Cl. The concentrated organics were purified by column chromatography (SiO_2, 50→100% EtOAc in DCM) to yield the desired compound *N*-(6-{2-[(1*S*)-1-cyclopropylethyl]-7-methyl-1-oxo-2,3-dihydro-1*H*-isoindol-5-yl}imidazo[1,2-*b*]pyridazin-2-yl)methanesulfonamide **24**. ^{1}H NMR (400 MHz, DMSO-d_6) δ 10.56 (s, 1H), 8.15 (dd, J = 9.5, 0.7 Hz, 1H), 8.06 (d, J = 1.3 Hz, 1H), 7.96 – 7.91 (m, 2H), 7.86 (d, J = 9.5 Hz, 1H), 4.58 (s, 2H), 3.63 – 3.52 (m, 1H), 3.19 (s, 3H), 2.73 – 2.68 (m, 3H), 1.30 (d, J = 6.9 Hz, 3H), 1.21 – 1.11 (m,

1H), 0.62 – 0.53 (m, 1H), 0.46 – 0.34 (m, 2H), 0.24 (p, *J* = 4.8 Hz, 1H). ESI MS $[M+H]^+$ for $C_{21}H_{23}N_5O_3S$, calcd. 426.2, found 426.0.

(2*S*)-*N*1-(6-{2-[(1*S*)-1-Cyclopropylethyl]-7-methyl-1-oxo-2,3-dihydro-1*H*-isoindol-5-yl}imidazo[1,2-*b*]pyridazin-2-yl)pyrrolidine-1,2-dicarboxamide (25). To a solution of 5-{2-aminoimidazo[1,2-*b*]pyridazin-6-yl}-2-[(1*S*)-1-cyclopropylethyl]-7-methyl-2,3-dihydro-1*H*-isoindol-1-one **11** (97 mg, 0.222 mmol), L-prolinamide (25.3 mg, 0.222 mmol), and diisopropylamine (0.160 mL, 0.888 mmol) in DCM (3.7 ml) was added a 0.1 M solution of triphosgene in DCM (22.4 mg, 0.075 mmol) dropwise. After 24 h, the reaction was incomplete, but was quenched with methanol and concentrated in vacuo. The resulting residue was purified by reverse-phase HPLC to yield the desired compound (2*S*)-*N*1-(6-{2-[(1*S*)-1-cyclopropylethyl]-7-methyl-1-oxo-2,3-dihydro-1*H*-isoindol-5-yl}imidazo[1,2-*b*]pyridazin-2-yl)pyrrolidine-1,2-dicarboxamide **25**. ^{1}H NMR (400 MHz, DMSO-d_6) δ 9.38 (s, 1H), 8.17 (d, *J* = 0.7 Hz, 1H), 8.12 – 8.00 (m, 2H), 7.91 (s, 1H), 7.80 (d, *J* = 9.5 Hz, 1H), 7.37 (s, 1H), 6.96 (d, *J* = 3.1 Hz, 1H), 4.58 (s, 2H), 4.34 – 4.27 (m, 1H), 3.69 – 3.56 (m, 1H), 3.59 – 3.42 (m, 1H), 2.71 (s, 3H), 2.14 – 2.01 (m, 1H), 1.94 – 1.84 (m, 3H), 1.29 (d, *J* = 6.8 Hz, 3H), 1.15 (dd, *J* = 8.9, 5.1 Hz, 1H), 0.63 – 0.53 (m, 1H), 0.45 – 0.34 (m, 2H), 0.29 – 0.19 (m, 1H). ESI MS $[M+H]^+$ for $C_{26}H_{29}N_7O_3$, calcd. 488.2, found 488.2.

5-{2-Amino-3-[1-(2-hydroxyethyl)-1*H*-pyrazol-4-yl]pyrazolo[1,5-*a*]pyrimidin-5-yl}-2-[(1*S*)-1-cyclopropylethyl]-7-methyl-2,3-dihydro-1*H*-isoindol-1-one (26). The title compound was prepared in a similar fashion to compound **17** using 2-[4-(4,4,5,5-tetramethyl-1,3,2-dioxaborolan-2-yl)-1*H*-pyrazol-1-yl]ethan-1-ol as the nucleophilic cross-coupling partner. The intermediate acetamide was hydrolyzed as described for compound **17**. ^{1}H NMR (400 MHz, chloroform-*d*) δ 8.42 (d, *J* = 7.2 Hz, 1H), 8.10 (s, 1H), 8.06 (s, 1H), 7.97 (s, 1H), 7.85 (s, 1H), 7.11 (d, *J* = 7.2 Hz, 1H), 4.62 – 4.43 (m, 2H), 4.40 – 4.26 (m, 4H), 4.15 – 4.05 (m, 2H), 3.83 – 3.71 (m, 1H), 3.28 – 3.14 (m, 1H), 2.82 (s, 3H), 1.37 (d, *J* = 6.8 Hz, 3H), 1.12 – 1.00 (m, 1H), 0.73 – 0.60 (m, 1H), 0.53 – 0.33 (m, 3H). ESI MS $[M+H]^+$ for $C_{25}H_{27}N_7O_2$, calcd. 458.2, found 458.2.

5-[2-Amino-3-(2-methyl-1,3-oxazol-5-yl)pyrazolo[1,5-*a*]pyrimidin-5-yl]-2-[(1*S*)-1-cyclopropylethyl]-7-methyl-2,3-dihydro-1*H*-isoindol-1-one (27). The title compound was prepared in a

similar fashion to compound **17** using 2-methyl-5-(4,4,5,5-tetramethyl-1,3,2-dioxaborolan-2-yl)-1,3-oxazole as the nucleophilic cross-coupling partner. The intermediate acetamide was hydrolyzed as described for compound **17**. ^{1}H NMR (400 MHz, DMSO-d_6) δ 8.90 (d, J = 7.1 Hz, 1H), 8.31 (s, 1H), 8.09 (s, 1H), 7.52 (d, J = 7.2 Hz, 1H), 7.37 (s, 1H), 4.61 (s, 2H), 3.67 – 3.54 (m, 1H), 2.72 (s, 3H), 2.51 (s, 3H) 1.30 (d, J = 6.8 Hz, 3H), 1.20 – 1.10 (m, 1H), 0.62 – 0.55 (m, 1H), 0.46 – 0.35 (m, 2H), 0.29 – 0.21 (m, 1H). ESI MS $[M+H]^+$ for $C_{24}H_{24}N_6O_2$, calcd. 429.2, found 429.2.

5-[2-Amino-3-(1*H*-pyrazol-5-yl)pyrazolo[1,5-*a*]pyrimidin-5-yl]-2-[(1*S*)-1-cyclopropylethyl]-7-methyl-2,3-dihydro-1*H*-isoindol-1-one (28). The title compound was prepared in a similar fashion to compound **17** using 1-(oxan-2-yl)-5-(4,4,5,5-tetramethyl-1,3,2-dioxaborolan-2-yl)-1*H*-pyrazole as the nucleophilic cross-coupling partner and $Pd(PPh_3)_4$ (10 mol%) as the catalyst. The intermediate acetamide was hydrolyzed as described for compound **17**, which occurred with concurrent THP group removal. ^{1}H NMR (400 MHz, DMSO-d_6) δ 8.84 (d, J = 7.1 Hz, 1H), 8.28 (s, 1H), 8.08 (s, 1H), 7.83 (d, J = 2.3 Hz, 1H), 7.41 (d, J = 7.1 Hz, 1H), 7.06 (d, J = 2.3 Hz, 1H), 4.60 (s, 2H), 3.70 – 3.51 (m, 1H), 2.71 (s, 3H), 1.28 (d, J = 6.8 Hz, 3H), 1.20 – 1.09 (m, 1H), 0.67 – 0.53 (m, 1H), 0.47 – 0.33 (m, 2H), 0.30 – 0.17 (m, 1H). ESI MS $[M+H]^+$ for $C_{23}H_{23}N_7O$, calcd. 414.2, found 414.2.

5-[2-Amino-3-(1*H*-1,2,4-triazol-3-yl)pyrazolo[1,5-*a*]pyrimidin-5-yl]-2-[(1*S*)-1-cyclopropylethyl]-7-methyl-2,3-dihydro-1*H*-isoindol-1-one (29). To a mixture of the isoindolinone boronate **44** (4.80 g, 20.0 mmol), ethyl 2-amino-5-chloropyrazolo[1,5-a]pyrimidine-3-carboxylate (6.83 g, 20.0 mmol), $PdCl_2$(dppf) (732 mg, 1.00 mmol), and K_2CO_3 (5.53 g, 40.0 mmol) under N_2 was added a degassed mixture of 4:1 dioxane: H_2O (100 mL). The reaction mixture was stirred at 100 °C for 1 h. Upon cooling, brine (20 mL) and 19:1 DCM:MeOH (500 mL) were added. The organic phase was dried over Na_2SO_4, concentrated, and purified twice by column chromatography (SiO_2, 0 → 10% MeOH in DCM) and (0 → 50% acetone in DCM) to afford ethyl 2-amino-5-{2-[(1*S*)-1-cyclopropylethyl]-7-methyl-1-oxo-2,3-dihydro-1*H*-isoindol-5-yl}pyrazolo[1,5-*a*]pyrimidine-3-carboxylate as a yellow solid (4.02 g, 48%).

To a mixture of ethyl 2-amino-5-{2-[(1*S*)-1-cyclopropylethyl]-7-methyl-1-oxo-2,3-dihydro-1*H*-isoindol-5-yl}pyrazolo[1,5-*a*]pyrimidine-3-carboxylate (4.02 g, 9.58 mmol) and EtOH (48 mL) at rt was

added LiOH (9.58 mL, 28.8 mmol, 3 M in H_2O). The reaction mixture was stirred at 80 °C for 1 h. The mixture was cooled and EtOH was removed under reduced pressure. H_2O (200 mL) was added and the mixture was acidified to pH 2-3 with 2 M aq. HCl (~14 mL). The solids were collected by filtration, washed with H_2O, and dried in vacuo to afford 2-amino-5-{2-[(1*S*)-1-cyclopropylethyl]-7-methyl-1-oxo-2,3-dihydro-1*H*-isoindol-5-yl}pyrazolo[1,5-*a*]pyrimidine-3-carboxylic acid as a yellow solid (3.49 g, 93%).

To a suspension of 2-amino-5-{2-[(1*S*)-1-cyclopropylethyl]-7-methyl-1-oxo-2,3-dihydro-1*H*-isoindol-5-yl}pyrazolo[1,5-*a*]pyrimidine-3-carboxylic acid (157 mg, 0.40 mmol) in DCM (1.2 mL, 0.34 M) was added NEt_3 (60 µL, 0.46 mmol) followed by $SOCl_2$ (40 µL, 0.44 mmol). The resulting mixture was stirred at 40 °C for 2 h, then at 25 °C for 14 h, during which time the product precipitated from solution. The mixture was diluted with hexanes (10 mL). The solid was collected by vacuum filtration, washed with DCM (2 x 5 mL), and dried in vacuo to afford 2-amino-5-{2-[(1*S*)-1-cyclopropylethyl]-7-methyl-1-oxo-2,3-dihydro-1*H*-isoindol-5-yl}pyrazolo[1,5-*a*]pyrimidine-3-carbonyl chloride as a beige solid (160 mg, 97% yield), which used directly in the next step without purification.

A portion of 2-amino-5-{2-[(1*S*)-1-cyclopropylethyl]-7-methyl-1-oxo-2,3-dihydro-1*H*-isoindol-5-yl}pyrazolo[1,5-*a*]pyrimidine-3-carbonyl chloride obtained in the previous step (120 mg, 0.29 mmol) in THF (15 mL) was slowly added to a well-stirred mixture of 28% NH_4OH (4.0 mL) and NH_4Cl (440 mg, 8.2 mmol) at 5 °C. The resulting mixture warmed to rt and stirred for 0.5 h. Upon completion, the organic phase was separated and the aqueous phase was back extracted with EtOAc. The combined organic extracts were dried (Na_2SO_4), filtered, and concentrated under reduced pressure to afford 2-amino-5-{2-[(1*S*)-1-cyclopropylethyl]-7-methyl-1-oxo-2,3-dihydro-1*H*-isoindol-5-yl}pyrazolo[1,5-*a*]pyrimidine-3-carboxamide as a beige solid (109 mg, 95% yield), which was used directly in the next step without purification.

A solution of 2-amino-5-{2-[(1*S*)-1-cyclopropylethyl]-7-methyl-1-oxo-2,3-dihydro-1*H*-isoindol-5-yl}pyrazolo[1,5-*a*]pyrimidine-3-carboxamide (109 mg, 0.28 mmol) in DMF-DMA (1.0 mL, 0.3 M) was stirred at 110 °C for 2 h. Upon completion, the reaction mixture was cooled to 25 °C and concentrated in vacuo to afford crude intermediate 5-{2-[(1*S*)-1-cyclopropylethyl]-7-methyl-1-oxo-2,3-dihydro-1*H*-

isoindol-5-yl}-*N*-[(*E*)-(dimethylamino)methylidene]-2-[(*E*)-[(dimethylamino)methylidene]amino]pyrazolo[1,5-*a*]pyrimidine-3-carboxamide as a brown oil. The crude product was dissolved in AcOH (0.8 mL) and hydrazine monohydrate (30 μL) was added. The resulting mixture was stirred at 90 °C for 1 h. Upon completion, the solution was cooled to 25 °C, concentrated in vacuo, and purified by column chromatography (SiO_2, 0 → 5% MeOH/DCM). The resulting material was subjected to a second purification by reverse-phase HPLC, which afforded 5-[2-amino-3-(1*H*-1,2,4-triazol-3-yl)pyrazolo[1,5-*a*]pyrimidin-5-yl]-2-[(1*S*)-1-cyclopropylethyl]-7-methyl-2,3-dihydro-1*H*-isoindol-1-one **29** as a beige solid. ^{1}H NMR (400 MHz, Chloroform-*d*) δ 8.51 (d, *J* = 7.1 Hz, 1H), 8.05 – 8.04 (m, 1H), 8.03 (s, 1H), 7.83 – 7.80 (m, 1H), 7.24 (d, *J* = 7.1 Hz, 1H), 5.62 (s, 2H), 4.70 – 4.45 (m, 2H), 3.86 – 3.72 (m, 1H), 2.85 (s, 3H), 1.38 (d, *J* = 6.8 Hz, 3H), 1.07 (m, 1H), 0.74 – 0.62 (m, 1H), 0.55 – 0.33 (m, 3H). ESI MS $[M+H]^+$ for $C_{22}H_{22}N_8O$, calcd. 415.2, found 415.1.

5-[2-Amino-3-(pyridin-2-yl)pyrazolo[1,5-*a*]pyrimidin-5-yl]-2-[(1*S*)-1-cyclopropylethyl]-7-methyl-2,3-dihydro-1*H*-isoindol-1-one (30). To a solution of iodide **55** (50 mg, 0.097 mmol) and 2-(tributylstannyl)pyridine (72 mg, 0.194 mmol) in DMF (1 mL) was added Pd_2dba_3 (7.1 mg, 0.0078 mmol) and XPhos (7.1 mg, 0.016 mmol). The resulting mixture was stirred at 135 °C for 1 h. Upon completion, the reaction was concentrated under reduced pressure and purified by column chromatography (SiO_2, DCM →5% MeOH/DCM) to afford intermediate cross-coupled acetamide that was hydrolyzed as described for compound **17**, which furnished the final compound 5-[2-amino-3-(pyridin-2-yl)pyrazolo[1,5-*a*]pyrimidin-5-yl]-2-[(1*S*)-1-cyclopropylethyl]-7-methyl-2,3-dihydro-1*H*-isoindol-1-one **30**. ^{1}H NMR (400 MHz, DMSO-d_6) δ 8.96 (d, *J* = 7.1 Hz, 1H), 8.74 – 8.68 (m, 1H), 8.57 (ddd, *J* = 4.9, 1.9, 0.9 Hz, 1H), 8.32 (s, 1H), 8.13 (s, 1H), 7.99 – 7.89 (m, 1H), 7.57 (d, *J* = 7.2 Hz, 1H), 7.22 – 7.12 (m, 1H), 4.63 (s, 2H), 3.68 – 3.54 (m, 1H), 2.75 (s, 3H), 1.31 (d, *J* = 6.8 Hz, 3H), 1.23 – 1.07 (m, 1H), 0.66 – 0.54 (m, 1H), 0.49 – 0.36 (m, 2H), 0.32 – 0.22 (m, 1H). ESI MS $[M+H]^+$ for $C_{25}H_{24}N_6O$, calcd. 425.2, found 425.2.

5-[2-Amino-3-(pyrimidin-4-yl)pyrazolo[1,5-*a*]pyrimidin-5-yl]-2-[(1*S*)-1-cyclopropylethyl]-7-methyl-2,3-dihydro-1*H*-isoindol-1-one (31). The title compound was prepared in a similar fashion to compound **30** using 4-(tributylstannyl)pyrimidine as the nucleophilic cross-coupling partner. The

intermediate cross-coupled acetamide was hydrolyzed as described for compound **17**. ^{1}H NMR (400 MHz, DMSO-d_6) δ 9.09 (dd, J = 1.4, 0.6 Hz, 1H), 9.05 (d, J = 7.1 Hz, 1H), 8.75 (dd, J = 5.8, 0.6 Hz, 1H), 8.66 (dd, J = 5.8, 1.4 Hz, 1H), 8.35 (s, 1H), 8.15 (s, 1H), 7.74 (d, J = 7.2 Hz, 1H), 4.64 (s, 2H), 3.66 – 3.56 (m, 1H), 2.75 (s, 3H), 1.31 (d, J = 6.9 Hz, 3H), 1.21 – 1.10 (m, 1H), 0.64 – 0.55 (m, 1H), 0.47 – 0.37 (m, 2H), 0.32 – 0.21 (m, 1H). ESI MS $[M+H]^+$ for $C_{24}H_{23}N_7O$, calcd. 426.2, found 426.2.

4-(2-Amino-5-{2-[(1*S*)-1-cyclopropylethyl]-7-methyl-1-oxo-2,3-dihydro-1*H*-isoindol-5-yl}pyrazolo[1,5-*a*]pyrimidin-3-yl)-2-methylbenzoic acid (32). The title compound was prepared in a similar fashion to compound **17** using [4-(methoxycarbonyl)-3-methylphenyl]boronic acid as the nucleophilic cross-coupling partner. The intermediate methyl 4-(5-{2-[(1*S*)-1-cyclopropylethyl]-7-methyl-1-oxo-2,3-dihydro-1*H*-isoindol-5-yl}-2-acetamidopyrazolo[1,5-*a*]pyrimidin-3-yl)-2-methylbenzoate (100 mg, 0.186 mmol) was treated with 6 M NaOH (aq.) (0.31 mL, 1.86 mmol), MeOH (0.5 mL) and THF (1 mL) and stirred at 70 °C for 2 h. Upon completion by LCMS analysis, the reaction was diluted with EtOAc (20 mL) and acidified with 2 M HCl (aq.) (10 mL). The aqueous layer was separated and back extracted with additional EtOAc (2 × 20 mL). The organic layers were combined, dried over $MgSO_4$ and concentrated under reduced pressure. Purification by reverse-phase HPLC furnished the desired compound 4-(2-amino-5-{2-[(1*S*)-1-cyclopropylethyl]-7-methyl-1-oxo-2,3-dihydro-1*H*-isoindol-5-yl}pyrazolo[1,5-*a*]pyrimidin-3-yl)-2-methylbenzoic acid **32**. ^{1}H NMR (400 MHz, DMSO-d_6) δ 8.90 (d, J = 7.2 Hz, 1H), 8.23 (s, 1H), 8.09 (s, 1H), 8.00 – 7.93 (m, 2H), 7.91 (s, 1H), 7.52 (d, J = 7.2 Hz, 1H), 4.60 (s, 2H), 3.64 – 3.53 (m, 1H), 2.72 (s, 3H), 2.64 (s, 3H), 1.30 (d, J = 6.8 Hz, 3H), 1.22 – 1.10 (m, 1H), 0.65 – 0.54 (m, 1H), 0.47 – 0.34 (m, 2H), 0.28 – 0.21 (m, 1H). ESI MS $[M+H]^+$ for $C_{28}H_{27}N_5O_3$, calcd. 482.2, found 482.2.

2-[4-(2-Amino-5-{2-[(1*S*)-1-cyclopropylethyl]-7-methyl-1-oxo-2,3-dihydro-1*H*-isoindol-5-yl}pyrazolo[1,5-*a*]pyrimidin-3-yl)phenyl]acetic acid (33). The title compound was prepared in a similar manner to compound **32** using 2-[4-(dihydroxyboranyl)phenyl]acetic acid as the nucleophilic cross-coupling partner, followed by NaOH-mediated hydrolysis/saponification. ^{1}H NMR (400 MHz, DMSO-d_6) δ 8.86 (d, J = 7.2 Hz, 1H), 8.21 (s, 1H), 8.04 (s, 1H), 7.91 – 7.83 (m, 2H), 7.45 (d, J = 7.2 Hz, 1H), 7.41 – 7.32 (m, 2H), 4.59 (s, 2H), 3.63 – 3.54 (m, 3H), 2.71 (s, 3H), 1.29 (d, J = 6.8 Hz, 3H), 1.20 – 1.09 (m, 1H),

0.63 – 0.53 (m, 1H), 0.47 – 0.34 (m, 2H), 0.30 – 0.20 (m, 1H). ESI MS $[M+H]^+$ for $C_{28}H_{27}N_5O_3$, calcd. 482.2, found 482.2.

***N*-(5-{2-[(1*S*)-1-Cyclopropylethyl]-1-oxo-7-(trifluoromethyl)-2,3-dihydro-1*H*-isoindol-5-yl}pyrazolo[1,5-*a*]pyrimidin-2-yl)acetamide (34)**. A mixture of 4-chloro-2-(trifluoromethyl)benzoic acid **56** (20.0 g, 89 mmol), (*S*)-1-cyclopropylethan-1-amine (9.32 g, 107 mmol), HATU (40.7 g, 107 mmol) and diisopropylethylamine (48 mL, 267 mmol) in anhydrous DMF (297 mL) was stirred at 23 °C for 2 h. The reaction mixture was quenched with *sat. aq.* NH_4Cl, extracted with EtOAc, evaporated and the crude product was purified by column chromatography (SiO_2, 0% → 40% gradient of EtOAc in Hexanes) to give 4-chloro-*N*-[(1*S*)-1-cyclopropylethyl]-2-(trifluoromethyl)benzamide **57** as a white solid (25.5 g, 98%). ESI MS $[M+H]^+$ for $C_{13}H_{13}ClF_3NO$, calcd. 292.1, found 292.1.

Intermediate **57** (8.20 g, 28 mmol) from the previous step was dissolved in THF (140 mL) and cooled to -78 °C, then *sec*-Butyllithium (1.4 M in cyclohexane, 50 mL, 70 mmol) was added dropwise. The reaction mixture was stirred at -78 °C for 20 min, then DMF (10.8 mL, 140 mmol) was added dropwise. After 1 h, the reaction was carefully quenched with *sat. aq.* NH_4Cl solution and extracted with EtOAc. After concentration, the crude product was dissolved in DCM (90 ml) and cooled to 0 °C. Et_3SiH (4.5 ml) and TFA (45 ml) were added and the reaction mixture was stirred at 23 °C for 20 mins. The reaction mixture was concentrated under reduced pressure, quenched with *sat. aq.* $NaHCO_3$ solution and extracted with DCM. The crude mixture was purified by column chromatography (SiO_2, 0 → 30% gradient of EtOAc in Hexanes) to give 5-chloro-2-[(1*S*)-1-cyclopropylethyl]-7-(trifluoromethyl)-2,3-dihydro-1*H*-isoindol-1-one as a white solid (7.15 g, 84%). ESI MS $[M+H]^+$ for $C_{14}H_{13}ClF_3NO$, calcd. 304.1, found 304.0.

A mixture of the product from the previous step (6.64 g, 21.9 mmol), B_2pin_2 (6.11 g, 24.0 mmol), KOAc (7.52 g, 76.7 mmol) and PCy3 Pd G2 (1.29 g, 2.19 mmol) in anhydrous dioxane (109 mL) was stirred at 100 °C for 1 h. The reaction mixture was filtered, concentrated under reduced pressure, and the crude product was purified by column chromatography (SiO_2, 0 → 30% gradient of EtOAc in Hexanes) to give 2-[(1*S*)-1-cyclopropylethyl]-5-(4,4,5,5-tetramethyl-1,3,2-dioxaborolan-2-yl)-7-(trifluoromethyl)-2,3-dihydro-1*H*-isoindol-1-one **58** as a brown solid (8.80 g, 94%).

A mixture of 2-[(1*S*)-1-cyclopropylethyl]-5-(4,4,5,5-tetramethyl-1,3,2-dioxaborolan-2-yl)-7-(trifluoromethyl)-2,3-dihydro-1*H*-isoindol-1-one **58** (68 mg, 0.173 mmol), chloride **53** (40 mg, 0.190 mmol), $PdCl_2$(dppf) (13 mg, 0.017 mol), 1 M Na_2CO_3 (aq.) (0.50 mL, 0.50 mmol) in dioxane (1.5 mL) was heated at 95 °C for 15 min. Upon completion, the reaction was partitioned between EtOAc (20 mL) and H_2O (20 mL). The aqueous layer was separated and back extracted with additional EtOAc (20 mL). The organic layers were combined, dried over $MgSO_4$, and concentrated under reduced pressure. Purification by reverse-phase HPLC gave *N*-(5-{2-[(1*S*)-1-cyclopropylethyl]-1-oxo-7-(trifluoromethyl)-2,3-dihydro-1*H*-isoindol-5-yl}pyrazolo[1,5-*a*]pyrimidin-2-yl)acetamide **34**. ^{1}H NMR (400 MHz, DMSO-d_6) δ 11.00 (s, 1H), 9.16 (dd, *J* = 7.3, 0.9 Hz, 1H), 8.73 (s, 1H), 8.58 (s, 1H), 7.77 (d, *J* = 7.4 Hz, 1H), 7.00 (s, 1H), 4.73 (s, 2H), 3.67 – 3.57 (m, 1H), 2.13 (s, 3H), 1.32 (d, *J* = 6.8 Hz, 3H), 1.24 – 1.13 (m, 1H), 0.69 – 0.54 (m, 1H), 0.51 – 0.35 (m, 2H), 0.33 – 0.23 (m, 1H). ^{13}C NMR (125 MHz, DMSO-d_6) δ 168.5, 163.1, 153.1, 152.8, 147.7, 145.5, 139.2, 135.8, 130.9, 126.1, 125.3, 123.8, 122.8, 105.0, 86.5, 52.0, 45.82, 23.4, 18.0, 15.5, 3.8, 3.4. ESI HRMS $[M+H]^+$ for $C_{22}H_{20}F_3N_5O_2$, calcd. 444.1642, found 444.1638.

***N*-(5-{2-[(1*S*)-1-Cyclopropylethyl]-7-methanesulfonamido-1-oxo-2,3-dihydro-1*H*-isoindol-5-yl}pyrazolo[1,5-*a*]pyrimidin-2-yl)acetamide (35)**. To a solution of 4-bromo-2-fluoro-6-methylbenzoic acid methyl ester **59** (45.0 g, 182 mmol) in CCl_4 (1.14 L) were added NBS (35.7 g, 200 mmol) and BPO (80 wt.%, 5.51 g, 18.2 mmol). The resulting mixture was stirred at reflux for 3 h. Upon completion, the reaction mixture was cooled to rt and filtered to remove the precipitate. The filtrate was concentrated in vacuo to afford the crude methyl 4-bromo-2-(bromomethyl)-6-fluorobenzoate **60** that was used directly in the next step.

In a round-bottom flask equipped with a reflux condenser and a balloon of N_2, crude methyl 4-bromo-2-(bromomethyl)-6-fluorobenzoate **60** (45.0 g, 138 mmol) was combined with (*S*)-1-cyclopropylethan-1-amine hydrochloride (33.6 g, 276 mmol), K_2CO_3 (57.2 g, 414 mmol) and $B(OH)_3$ (1.71 g, 27.6 mmol) in CH_3CN (552 mL). The resulting mixture was stirred at 50 °C for 72 h. Upon completion, the reaction mixture was cooled to rt and ~75% of the solvent was removed in vacuo. The mixture was partitioned between EtOAc (300 mL) and H_2O (200 mL). The aqueous phase was separated and extracted

with additional EtOAc (300 mL). The combined organic extracts were washed with H_2O and brine, then dried (Na_2SO_4), filtered and concentrated in vacuo. Purification by column chromatography (SiO_2, 0 → 30% gradient EtOAc/hexanes) afforded 5-bromo-2-[(1*S*)-1-cyclopropylethyl]-7-fluoro-2,3-dihydro-1*H*-isoindol-1-one **61** as an off-white solid (35.0 g, 58% yield over 2 steps). ESI MS $[M+H]^+$ for $C_{13}H_{13}BrFNO$, calcd. 298.0, found 298.0

Intermediate **61** (3.00 g, 10.0 mmol) was combined with neat $PMBNH_2$ (4 mL) and heated to 100 °C for 14 h. The reaction mixture was cooled and partitioned between 10% aq. citric acid solution and EtOAc. The aqueous layer was separated and back extracted with additional EtOAc. The organic layers were combined and washed with additional 10% aq. citric acid solution, brine, and dried over $MgSO_4$. Concentration under reduced pressure furnished 5-bromo-2-[(1*S*)-1-cyclopropylethyl]-7-{[(4-methoxyphenyl)methyl]amino}-2,3-dihydro-1*H*-isoindol-1-one **62** that was used crude in the next step.

Crude 5-bromo-2-[(1*S*)-1-cyclopropylethyl]-7-{[(4-methoxyphenyl)methyl]amino}-2,3-dihydro-1*H*-isoindol-1-one **62** was combined with TFA (15 mL) and stirred at 40 °C for 3 h. The reaction mixture was concentrated under reduced pressure and quenched with *sat*. *aq*. $NaHCO_3$ solution and diluted with EtOAc. The organic layers were combined, washed with brine and dried over $MgSO_4$. Concentration under reduced pressure and purification by column chromatography (SiO_2, 0 → 50% EtOAc/hexane) furnished 7-amino-5-bromo-2-[(1*S*)-1-cyclopropylethyl]-2,3-dihydro-1*H*-isoindol-1-one **63** as a white solid (2.89 g, ~98%, minor impurity co-eluted that was taken forward in the next step). ESI MS $[M+H]^+$ for $C_{13}H_{15}BrN_2O$, calcd. 295.0, found 295.0.

7-Amino-5-bromo-2-[(1*S*)-1-cyclopropylethyl]-2,3-dihydro-1*H*-isoindol-1-one **63** (1.00 g, 3.38 mmol) was dissolved in DCM (10 mL) and the mixture was cooled to 0 °C. To this solution was added DMAP (40 mg, 0.34 mmol), DIPEA (1.6 mL, 10.1 mmol) and MsCl (0.7 mL, 8.5 mmol). The reaction mixture was warmed to rt and stirred for 1 h. The reaction was quenched with 1 M HCl (aq.) and diluted with EtOAc. The aqueous layer was separated and back extracted with additional EtOAc. The organic layers were combined, washed with brine and dried over $MgSO_4$. Concentration under reduced pressure furnished bis-sulfonylated product that was taken crude into the next step.

Crude product from the previous step was dissolved in THF (5 mL) and TBAF (1.0 M in THF, 5.4 mL, 5.4 mmol) was added. An additional portion of TBAF (1.0 M in THF, 3.0 mL) was added after 15 min, followed by a final portion of TBAF (1.0 M in THF, 3.0 mL) after 2 h. The reaction mixture was stirred for an additional 1 h, then quenched with 1 M HCl (aq.) and diluted with EtOAc. The aqueous layer was separated and back extracted with additional EtOAc. The organic layers were combined, washed with brine and dried over $MgSO_4$. Concentration under reduced pressure and purification by column chromatography (SiO_2, 0 → 50% EtOAc/hexane) furnished *N*-{6-bromo-2-[(1*S*)-1-cyclopropylethyl]-3-oxo-2,3-dihydro-1*H*-isoindol-4-yl}methanesulfonamide as a yellow solid **64** (0.766 g, 60% over 2 steps). ESI MS $[M+H]^+$ for $C_{14}H_{17}BrN_2O_3S$, calcd. 373.0, found 373.0.

Miyaura borylation and cross-coupling (as described for compound **34**) gave *N*-(5-{2-[(1*S*)-1-cyclopropylethyl]-7-methanesulfonamido-1-oxo-2,3-dihydro-1*H*-isoindol-5-yl}pyrazolo[1,5-*a*]pyrimidin-2-yl)acetamide **35**. ^{1}H NMR (400 MHz, DMSO-d_6) δ 10.97 (s, 1H), 9.64 (s, 1H), 9.10 (dd, J = 7.3, 0.9 Hz, 1H), 8.16 (d, J = 1.2 Hz, 1H), 8.09 (d, J = 1.1 Hz, 1H), 7.56 (d, J = 7.4 Hz, 1H), 6.96 (s, 1H), 4.69 (s, 2H), 3.61 – 3.48 (m, 1H), 3.31 (s, 3H), 2.12 (s, 3H), 1.33 (d, J = 6.8 Hz, 3H), 1.22 – 1.13 (m, 1H), 0.65 – 0.53 (m, 1H), 0.50 – 0.34 (m, 2H), 0.32 – 0.21 (m, 1H). ESI MS $[M+H]^+$ for $C_{22}H_{24}N_6O_4S$, calcd. 469.2, found 469.0.

***N*-(5-{2-[(1*S*)-1-Cyclopropylethyl]-7-(methylsulfamoyl)-1-oxo-2,3-dihydro-1*H*-isoindol-5-yl}pyrazolo[1,5-*a*]pyrimidin-2-yl)acetamide (36)**. To a solution of 5-bromo-2-[(1*S*)-1-cyclopropylethyl]-7-fluoro-3*H*-isoindol-1-one **61** (2.50 g, 8.4 mmol) and benzyl mercaptan (1.18 mL, 10.1 mmol) in DMF (28 mL) was added potassium carbonate (3.47 g, 25.2 mmol). The mixture was heated to 50 °C overnight. After cooling to room temperature, the reaction was partitioned between EtOAc and water. The organics were washed with water (3x) and brine then dried over $MgSO_4$ and the solvent removed under reduced pressure. Purification by column chromatography (SiO_2, 10 → 50% EtOAc/hexanes) afforded **65** (1.88 g, 56% yield). ESI MS $[M+H]^+$ for $C_{20}H_{20}BrNOS$, calcd. 402.0, found 402.0.

To a solution of 7-benzylsulfanyl-5-bromo-2-[(1*S*)-1-cyclopropylethyl]-3*H*-isoindol-1-one **65** (1.88 g, 4.68 mmol) in acetic acid (28 mL) and H_2O (3 mL) was added *N*-chlorosuccinimide (1.87 g, 14.0

mmol). The reaction was stirred at room temperature for two hours then diluted with EtOAc and washed with water (2x) and brine. The organics were dried over $MgSO_4$ and concentrated under reduced pressure to provide crude 6-bromo-2-[(1*S*)-1-cyclopropylethyl]-3-oxo-1*H*-isoindole-4-sulfonyl chloride which was used without further purification.

To a solution of crude 6-bromo-2-[(1*S*)-1-cyclopropylethyl]-3-oxo-1*H*-isoindole-4-sulfonyl chloride (758 mg, 2.0 mmol) in DCM (16 mL) was added methylamine hydrochloride (270 g, 4.0 mmol) followed by pyridine (2.7 mL) and DIPEA (697 µL, 4.0 mmol). After 2 h, the reaction was diluted with EtOAc and washed sequentially with 0.2 M HCl (aq.), water, and brine. The organics were dried over $MgSO_4$ and concentrated under reduced pressure. Purification by column chromatography (SiO_2, 20 → 70% EtOAc/hexanes) afforded the desired product **66** (500 mg, 67% yield) as an off-white solid. ESI MS [M+H]+ for $C_{14}H_{17}BrN_2O_3S$, calcd. 373.0, found 373.0.

A flask charged with *N*-(5-chloropyrazolo[1,5-*a*]pyrimidin-2-yl)acetamide **53** (1.50 g, 7.12 mmol), bis(pinacolato)diboron (2.17 g, 8.54 mmol), potassium acetate (1.74 g, 17.8 mmol) and $PdCl_2$(dppf) (519 mg, 0.71 mmol) was evacuated and backfilled with nitrogen (2x) then degassed dioxane (17.8 mL) was added and the sealed vial was heated to 100 °C for 3 h. After cooling to rt, the reaction mixture was filtered through celite and the filter pad was washed with 15% MeOH/DCM (25 mL). Et_2O (150 mL) was added to the filtrate to precipitate **67** (1.2 g, 56%) which was used without further purification.

A vial charged with 6-bromo-2-[(1*S*)-1-cyclopropylethyl]-*N*-methyl-3-oxo-1*H*-isoindole-4-sulfonamide **66** (100 mg, 0.27 mmol), *N*-[6-(4,4,5,5-tetramethyl-1,3,2-dioxaborolan-2-yl)imidazo[1,2-*b*]pyridazin-2-yl]acetamide **67** (105 mg, 0.35 mmol), and $PdCl_2$(dppf) (20 mg, 0.03 mmol) was evacuated and backfilled with nitrogen three times then degassed dioxane (2.7 mL) and 1.0 M Na_2CO_3 (aq.) (1.1 mL, 1.08 mmol) was added via syringe. The sealed vial was heated to 100 °C for 2 h. After cooling to rt, the reaction was diluted with EtOAc then washed with water and brine. The organics were dried over $MgSO_4$ and concentrated under reduced pressure. Purification by column chromatography (SiO_2, 0 → 10% MeOH/DCM) afforded *N*-(5-{2-[(1*S*)-1-cyclopropylethyl]-7-(methylsulfamoyl)-1-oxo-2,3-dihydro-1*H*-isoindol-5-yl}pyrazolo[1,5-*a*]pyrimidin-2-yl)acetamide **36** (40 mg, 32% yield) as an off-white solid. ESI

MS $[M+H]^+$ for $C_{22}H_{24}N_6O_4S$, calcd. 469.2, found 469.0. ^1H NMR (400 MHz, DMSO-*d6*) δ 10.98 (s, 1H), 8.58 (d, *J* = 1.5 Hz, 1H), 8.52 (d, *J* = 1.5 Hz, 1H), 8.37 (s, 1H), 8.16 (dd, *J* = 9.4, 0.7 Hz, 1H), 7.91 (d, *J* = 9.5 Hz, 1H), 7.57 (q, *J* = 5.1 Hz, 1H), 4.79 (s, 2H), 3.71 – 3.58 (m, 1H), 3.31 (s, 3H), 2.11 (s, 3H), 1.33 (d, *J* = 6.8 Hz, 3H), 1.29 – 1.07 (m, 1H), 0.67 – 0.54 (m, 1H), 0.51 – 0.37 (m, 2H), 0.34 – 0.21 (m, 1H).

5-[2-Amino-3-(1-methyl-1*H*-pyrazol-4-yl)pyrazolo[1,5-*a*]pyrimidin-5-yl]-2-[(1*S*)-1-cyclopropylethyl]-7-(trifluoromethyl)-2,3-dihydro-1*H*-isoindol-1-one (4). A mixture of 2-bromo-5-chloropyrazolo[1,5-*a*]pyrimidine **68** (600 mg, 2.58 mmol), 2-[(1*S*)-1-cyclopropylethyl]-5-(4,4,5,5-tetramethyl-1,3,2-dioxaborolan-2-yl)-7-(trifluoromethyl)-2,3-dihydro-1*H*-isoindol-1-one **58**, $PdCl_2$(dppf) 151 mg, 0.206 mmol) and 1 M Na_2CO_3 (aq.) (8.0 mL, 24 mmol), in dioxane (10 mL) was heated at 80 °C and stirred for 15 min. The reaction was cooled and partitioned between EtOAc (100 mL) and H_2O (100 mL). The aqueous phase was separated and back extracted with additional EtOAc (100 mL). The organic layers were combined, dried over $MgSO_4$, and concentrated under reduced pressure. Purification by column chromatography (SiO_2, DCM → 50% EtOAc/DCM) gave 5-{2-bromopyrazolo[1,5-*a*]pyrimidin-5-yl}-2-[(1*S*)-1-cyclopropylethyl]-7-(trifluoromethyl)-2,3-dihydro-1*H*-isoindol-1-one **69** (831 mg, 69%). ESI MS $[M+H]^+$ for $C_{20}H_{16}BrF_3N_4O$, calcd. 465.1, found 465.0.

A mixture of 5-{2-bromopyrazolo[1,5-*a*]pyrimidin-5-yl}-2-[(1*S*)-1-cyclopropylethyl]-7-(trifluoromethyl)-2,3-dihydro-1*H*-isoindol-1-one **69** (500 mg, 1.07 mmol), acetamide (190 mg, 3.22 mmol), BrettPhos Pd Gen3 (97 mg, 0.107 mmol), BrettPhos (115 mg, 0.214 mmol), Cs_2CO_3 (1.05 g, 3.22 mmol) in dioxane (8.2 mL) was heated at 100 °C and stirred for 90 min. The reaction was cooled, filtered and concentrated under reduced pressure. Purification by column chromatography (SiO_2, DCM → 10% MeOH/DCM) gave *N*-(5-{2-[(1*S*)-1-cyclopropylethyl]-1-oxo-7-(trifluoromethyl)-2,3-dihydro-1*H*-isoindol-5-yl}pyrazolo[1,5-*a*]pyrimidin-2-yl)acetamide **34** (284 mg, 60%).

To a solution of *N*-(5-{2-[(1*S*)-1-cyclopropylethyl]-1-oxo-7-(trifluoromethyl)-2,3-dihydro-1*H*-isoindol-5-yl}pyrazolo[1,5-*a*]pyrimidin-2-yl)acetamide **34** (284 mg, 0.640 mmol) in CH_3CN (4.3 mL) was added NIS (230 mg, 1.02 mmol). The resulting mixture was stirred at rt for 2 h. Concentration under reduced

pressure and purification by column chromatography (SiO_2, DCM → 10% DCM/MeOH gradient) gave *N*-(5-{2-[(1*S*)-1-cyclopropylethyl]-1-oxo-7-(trifluoromethyl)-2,3-dihydro-1*H*-isoindol-5-yl}-3-iodopyrazolo[1,5-*a*]pyrimidin-2-yl)acetamide **70** (320 mg, 88%). ESI MS $[M+H]^+$ for $C_{22}H_{19}F_3IN_5O_2$, calcd. 570.1, found 570.0.

5-[2-Amino-3-(1-methyl-1*H*-pyrazol-4-yl)pyrazolo[1,5-*a*]pyrimidin-5-yl]-2-[(1*S*)-1-cyclopropylethyl]-7-(trifluoromethyl)-2,3-dihydro-1*H*-isoindol-1-one **4** was prepared in two additional steps from iodide **70** following a similar protocol to that described for compound **17**. ^{1}H NMR (400 MHz, DMSO-d_6) δ 8.88 (d, J = 7.1 Hz, 1H), 8.76 (s, 1H), 8.60 (s, 1H), 8.22 (s, 1H), 8.13 (s, 1H), 7.52 (d, J = 7.2 Hz, 1H), 4.76 (s, 2H), 3.93 (s, 3H), 3.69 – 3.54 (m, 1H), 1.33 (d, J = 6.8 Hz, 3H), 1.25 – 1.12 (m, 1H), 0.67 – 0.55 (m, 1H), 0.53 – 0.36 (m, 2H), 0.31 – 0.22 (m, 1H). ESI HRMS $[M+H]^+$ for $C_{24}H_{22}F_3N_7O$, calcd. 482.1911, found 482.1910.

5-[2-Amino-3-(1,5-dimethyl-1*H*-pyrazol-4-yl)pyrazolo[1,5-*a*]pyrimidin-5-yl]-2-[(1*S*)-1-cyclopropylethyl]-7-(trifluoromethyl)-2,3-dihydro-1*H*-isoindol-1-one (37). The title compound was prepared from iodide **70** in analogous fashion to that described for compound **17** using 1,5-dimethyl-4-(4,4,5,5-tetramethyl-1,3,2-dioxaborolan-2-yl)-1*H*-pyrazole as the nucleophilic cross-coupling partner, followed by acetamide hydrolysis. ^{1}H NMR (400 MHz, DMSO-d_6) δ 8.87 (d, J = 7.1 Hz, 1H), 8.62 (s, 1H), 8.52 (d, J = 1.3 Hz, 1H), 7.55 – 7.43 (m, 2H), 4.71 (s, 2H), 3.82 (s, 3H), 3.67 – 3.54 (m, 1H), 2.33 (s, 3H), 1.31 (d, J = 6.8 Hz, 3H), 1.16 (dd, J = 8.8, 4.7 Hz, 1H), 0.64 – 0.53 (m, 1H), 0.41 (ddp, J = 14.4, 9.3, 5.2 Hz, 2H), 0.29 – 0.23 (m, 1H). ESI MS $[M+H]^+$ for $C_{25}H_{24}F_3N_7O$, calcd. 496.2, found 496.1.

5-[2-Amino-3-(1,3-dimethyl-1*H*-pyrazol-4-yl)pyrazolo[1,5-*a*]pyrimidin-5-yl]-2-[(1*S*)-1-cyclopropylethyl]-7-(trifluoromethyl)-2,3-dihydro-1*H*-isoindol-1-one (38). The title compound was prepared from iodide **70** in analogous fashion to that described for compound **17** using 1,3-dimethyl-4-(4,4,5,5-tetramethyl-1,3,2-dioxaborolan-2-yl)-1*H*-pyrazole as the nucleophilic cross-coupling partner, followed by acetamide hydrolysis. ^{1}H NMR (400 MHz, DMSO-d_6) δ 8.86 (d, J = 7.1 Hz, 1H), 8.62 (s, 1H), 8.54 (d, J = 1.4 Hz, 1H), 7.75 (s, 1H), 7.47 (d, J = 7.2 Hz, 1H), 4.71 (s, 2H), 3.83 (s, 3H), 3.66 – 3.54 (m, 1H), 2.24 (s, 3H), 1.30 (d, J = 6.8 Hz, 3H), 1.15 (td, J = 8.5, 8.1, 4.3 Hz, 1H), 0.58 (dq, J = 8.7, 4.4, 3.5 Hz,

1H), 0.41 (ddp, *J* = 14.4, 9.3, 5.0 Hz, 2H), 0.31 – 0.21 (m, 1H). ESI MS $[M+H]^+$ for $C_{25}H_{24}F_3N_7O$, calcd. 496.2, found 496.1.

5-[2-Amino-3-(pyrimidin-2-yl)pyrazolo[1,5-*a*]pyrimidin-5-yl]-2-[(1*S*)-1-cyclopropylethyl]-7-(trifluoromethyl)-2,3-dihydro-1*H*-isoindol-1-one (39). The title compound was prepared from iodide **70** in a similar fashion to compound **30** using 2-(tributylstannyl)pyrimidine as the nucleophilic cross-coupling partner, followed by acetamide hydrolysis. ^{1}H NMR (400 MHz, DMSO-d_6) δ 9.03 (d, *J* = 7.1 Hz, 1H), 8.84 (d, *J* = 4.9 Hz, 2H), 8.78 (s, 2H), 7.77 (d, *J* = 7.1 Hz, 1H), 7.21 (t, *J* = 4.9 Hz, 1H), 4.76 (s, 2H), 3.68 – 3.58 (m, 1H), 1.33 (d, *J* = 6.8 Hz, 3H), 1.25 – 1.13 (m, 1H), 0.66 – 0.56 (m, 1H), 0.49 – 0.37 (m, 2H), 0.33 – 0.24 (m, 1H). ESI MS $[M+H]^+$ for $C_{24}H_{20}F_3N_7O$, calcd. 480.2, found 480.2.

4-(2-Amino-5-{2-[(1*S*)-1-cyclopropylethyl]-1-oxo-7-(trifluoromethyl)-2,3-dihydro-1*H*-isoindol-5-yl}pyrazolo[1,5-*a*]pyrimidin-3-yl)-2-(propan-2-yl)benzoic acid (40). The title compound was prepared from iodide **70** in a similar fashion to compound **17** using 2-(propan-2-yl)-4-(4,4,5,5-tetramethyl-1,3,2-dioxaborolan-2-yl)benzoic acid as the nucleophilic cross-coupling partner, followed by acetamide hydrolysis. ^{1}H NMR (400 MHz, DMSO-d_6) δ 8.99 (d, *J* = 7.1 Hz, 1H), 8.71 (s, 1H), 8.65 (s, 1H), 8.23 (d, *J* = 1.7 Hz, 1H), 7.80 (d, *J* = 8.2 Hz, 1H), 7.69 (dd, *J* = 8.2, 1.8 Hz, 1H), 7.63 (d, *J* = 7.2 Hz, 1H), 4.71 (s, 2H), 3.94 (p, *J* = 6.6 Hz, 1H), 3.68 – 3.55 (m, 1H), 1.32 (d, *J* = 6.8 Hz, 3H), 1.30 (d, *J* = 6.8 Hz, 6H), 1.23 – 1.12 (m, 1H), 0.64 – 0.56 (m, 1H), 0.49 – 0.36 (m, 2H), 0.32 – 0.23 (m, 1H). ESI MS $[M+H]^+$ for $C_{30}H_{28}F_3N_5O_3$, calcd. 564.2, found 564.1.

4-(5-{2-[(1*S*)-1-Cyclopropylethyl]-1-oxo-7-(trifluoromethyl)-2,3-dihydro-1*H*-isoindol-5-yl}pyrazolo[1,5-*a*]pyrimidin-3-yl)-2-(propan-2-yl)benzoic acid (41). The title compound was prepared in a similar fashion to compound **14** using 3-bromo-5-chloropyrazolo[1,5-*a*]pyrimidine **49** as the starting material and iterative cross-couplings with isoindolinone boronate **58**, followed by 2-(propan-2-yl)-4-(4,4,5,5-tetramethyl-1,3,2-dioxaborolan-2-yl)benzoic acid. ^{1}H NMR (500 MHz, DMSO-d_6) δ 12.82 (s, 1H), 9.36 (d, *J* = 7.4 Hz, 1H), 8.92 (s, 1H), 8.79 (s, 1H), 8.75 (s, 1H), 8.56 (d, *J* = 1.8 Hz, 1H), 7.96 (dd, *J* = 8.2, 1.8 Hz, 1H), 7.92 (d, *J* = 7.4 Hz, 1H), 7.80 (d, *J* = 8.2 Hz, 1H), 4.74 (s, 2H), 3.99 – 3.86 (m, 1H), 3.70 – 3.57 (m, 1H), 1.38 – 1.28 (m, 9H), 1.25 – 1.16 (m, 1H), 0.65 – 0.57 (m, 1H), 0.49 – 0.37 (m, 2H), 0.32 –

0.25 (m, 1H).. ^{13}C NMR (125 MHz, DMSO-d_6) δ 169.1, 163.0, 153.9, 149.6, 145.6, 144.1, 144.0, 139.0, 137.5, 135.0, 131.2, 130.3, 127.9, 126.5, 125.5, 123.8, 123.2, 122.8, 122.5, 109.1, 106.2, 52.1, 45.8, 28.7, 23.8, 17.9, 15.5, 3.8, 3.4. ESI HRMS $[M+H]^+$ for $C_{30}H_{27}F_3N_4O_3$, calcd. 549.2108, found 549.2105.

Inhibition of PI3K Kinase Activity (Biochemical Assays). Compounds were evaluated to determine the potency with which they inhibited the kinase activity of the Class I PI3K subunits p110α/p85α (Promega, catalog # V1721), p110β/p85α (Promega, catalog # V1751), p120γ (Promega, catalog # V1761) and p110δ/p85α (Promega, catalog # V1771). Activity was determined as a function of adenosine diphosphate (ADP) generated from adenosine triphosphate (ATP) consumed during the phosphorylation of phosphatidylinositol-4,5-bisphosphate (PIP2) (Promega, catalog # V1701) to yield phosphatidylinositol-3,4,5-trisphosphate (PIP3). ADP levels in the assay mixture at the end of the reaction were quantitated using ADP Glo (Promega, catalog # V9103) according to the manufacturer's recommended protocol. On the day of the assay, compounds were solubilized in DMSO and dispensed into a 384-well white Opti-plate (PerkinElmer, catalog # 6007290) to generate a 14 point 1:2 titration. Enzyme was prepared for each of the PI3K subunits in 100 mM HEPES, pH 7.4, 100 mM NaCl, 6 mM MgCl2 and 0.05% BSA. p110α/p85α was prepared at 2 nM (2x), p110β/p85α was prepared at 7 nM (2x), p120γ was prepared at 8 nM (2x) and p110δ/p85α was prepared at 2 nM (2x). Five microliters of 2x enzyme dilution of each PI3K subunit were added to a 384-well white Opti-plate pre-dispensed with compound and allowed to incubate for 1 h at rt. A substrate mix containing 0.1 mg/mL (2x) of PIP2 and 50 μM (2x) ATP (Promega, catalog # V915) was prepared in 25 mM HEPES and 0.5 mM EGTA. Reactions were initiated by addition of 5 μL of 2x substrate mix to each well of the plates containing the various PI3K isoforms and allowed to proceed for 60 minutes at rt. Ten microliters of ADP Glo reagent 1 were added to the wells of each plate and allowed to incubate at rt for 45 minutes according to the manufacturer's directions. Following incubation, 20 μL of ADP Glo reagent 2 were added to each plate and allowed to incubate for an additional 45 minutes. Luminescent signal, generated by ADP Glo, was quantified by reading on a PerkinElmer Envision multimode reader. Compound potencies (IC_{50} values) were determined using a standard 4-parameter fit non-linear regression fit.

PI3Kγ Cellular Assay in THP-1 Cells. The day prior to assay, THP-1 cells (ATCC, catalog # TIB-202) were seeded at a density of 1×10^6 cells per mL in serum-free DMEM in a T175 flask (Thermo Fisher, catalog # 12-562-000) and incubated overnight at 5% CO_2 and 37 °C. On the day of experiment, a 14 point, 1:2 titration of test compound was pre-dispensed into 384 well Opti-plates (PerkinElmer, catalog # 6007290). Twenty microliters of serum-starved THP-1 cells were added to the compound plate in serum-free DMEM at a density of 9×10^6 cells per mL. Final assay conditions comprised 1.8×10^5 THP-1 cells per well with test compounds in 2% DMSO across a concentration range from 4 nM to 30 μM. Following a 60-minute incubation with test compound at 37 °C and 5% CO_2, THP-1 cells were stimulated with 25 nM rhMCP-1 (R&D Systems, catalog # 279-MC-010) for 2 minutes at 37 °C. PI3Kγ-stimulated phosphorylation of endogenous AKT Serine residue 473 in THP-1 cells was measured using an AlphaLISA SureFire Ultra AKT 1/2/3 (pS473) Assay Kit (PerkinElmer, catalog # ALSU-PAKT-B50K) according to the manufacturer's recommended protocol. Briefly, 10 μL of 4x lysis buffer were added to cells after stimulation. Following a 60-minute incubation at rt, 10 μL of cell lysate were transferred to a fresh 384-well Opti plate to which 5 μL of AlphaLisa acceptor beads and 5 μL of AlphaLisa donor beads had been added. After a further 120-minute incubation at rt in the dark, AlphaLisa signal was assessed using an Envision 2102 Multilabel Reader. PI3Kγ activity was evaluated as a correlate of endogenous AKT phosphorylation levels. Percentage maximum activity in each test well was calculated based on DMSO (100% activity) and positive control treated cell wells (0% activity). The potencies (IC_{50} values) of test compounds were determined using a standard 4-parameter fit non-linear regression fit.

Hepatocyte Stability Procedure. A 50-donor pool of cryopreserved human hepatocytes was thawed in prewarmed 37 °C thawing medium (BioIVT), centrifuged, and resuspended in incubation medium (BioIVT). The number of viable cells was determined by the Trypan blue exclusion method. The cells were diluted to 2 million viable cells/mL (viability >80%) and seeded into round-bottom 96-well plates (50 μL/well). The test compounds were dissolved in DMSO and further diluted in 50% acetonitrile, with a final concentration of 0.01% DMSO and 0.1% acetonitrile. Incubation was performed at a final concentration of 1 million cells/mL and 0.5 μM test compound, with agitation at a frequency of 1100 rpm

in a 37 °C, 5/95% CO_2/air incubator. At different time points, 100 μL samples were taken and mixed with 300 μL of ice-cold acetonitrile to stop the enzymatic reaction. After centrifugation at 4200 rpm, the supernatant was analyzed by LC-MS/MS.

CYP Inhibition Procedure. Test compounds were evaluated in vitro for their potential to inhibit major human drug metabolizing enzymes of the cytochrome P450 family. The test compounds were incubated separately over a concentration range of 0−40 μM with 0.1 mg/mL human liver microsomal protein suspension in 0.1 M potassium phosphate buffer at pH 7.4, 1 mM NADPH, and a probe substrate (Phenacetin for CYP1A2, Diclofenac for CYP2C9, S-mephenytoin for CYP2C19, dextromethorphan for CYP2D6, and midazolam for CYP3A4). Each substrate was incubated at 37 °C for 5−20 min as defined by the previous assay validation. Samples for each substrate were collected and pooled with samples from other substrate incubations for determination of product formation by LC-MS/MS. IC_{50} values were calculated using a variable slope (4-parameter) model. Furafylline (1A2), sulfaphenazole (2C9), (+)-N-3-benzylnirvanol (2C19), quinidine (2D6), and ketoconazole (3A4) were used as reference controls.

Rat Pharmacokinetics Determination. Pharmacokinetic properties in male SD rats (weight between 200 and 250 g) were determined following intravenous (IV) administration at a dose of 0.25 mg/kg. For IV dosing (n = 2 each group), rats were catheterized in jugular and femoral vein. Compounds were formulated in DMAC : EtOH : PG (31.6 : 36.8 : 31.6) for IV. Rats were not fasted during this study. Blood was sampled at 0 (pre-dose), 0.083, 0.25, 0.5, 1, 2, 4, 6 and 8 h following IV dosing. Plasma was isolated by centrifugation, and all samples were frozen at −80 °C. Calibration standards and QCs were prepared by the addition of known concentrations of compound to blank rat plasma to provide a calibration range of 0.5−5,000 ng/mL. Then, 50 μL plasma samples or calibration standard was added to 150 μL of internal standard solution in acetonitrile. Samples were vortex mixed and centrifuged at 4,200 rpm for 10 min at 4 °C. Supernatant (80 μL) was transferred to a 96 well injection plate containing 160 μL of water, mixed, and analyzed by LC-MS/MS. A bioanalytical method was developed for the quantification of compound in rat plasma. Method development and sample analysis was conducted using an API 6500 LC-MS/MS (Applied Biosystems, Foster City, CA) equipped with Shimadzu Nexera X2 UHPLC system (Shimadzu Scientific

Instruments, Maryland, MD). One μL of the samples was analyzed using a C18 reversed-phase column (Phenomenex Kinetex C18, 1.7 μm, 2.1 mm × 50.0 mm) (Phenomenex, Torrance, CA) interfaced to a Turbo Spray ionization source. Mobile phase consisted of A: water with 0.1% formic acid and B: acetonitrile with 0.1% formic acid. The flow rate was 0.5 mL/min and the gradient was 30% A to 100% B over 1.5 min and then 100% B for 1 min. Multiple reaction monitoring (MRM) transition (478.0/346.0 for internal standard) in positive ion mode was used. All animal experiments performed in the manuscript were conducted in compliance with the regulations of the Animal Care and Use Committee of Arcus Biosciences.

Crystallization and structure determination of IPI-549 3 bound to recombinant hPI3Kγ. Expression and purification of hPI3Kγ was performed according to previously established protocols, using affinity and gel filtration chromatography to yield homogeneous protein with >95% purity (Coomassie stained SDS-PAGE). The purified protein was crystallized to form apo-crystals using previously established conditions. Apo-crystals were used in soaking experiments with IPI-549 **3** (Ark Pharm, Inc., Catalog Number AK66292; 1 mM ligand for 2 h followed by 10 mM for 0.5 h). Crystals were flash-frozen and analyzed at a temperature of 100 K. Diffraction data of the complex crystals were collected at the Swiss Light Source (SLS, Villigen, Switzerland) and the structure was solved and refined to a final resolution of 2.99 Å. Data were processed using XDS and XSCALE. The crystals contained one monomer of hPI3Kγ in the asymmetric unit and the model comprises residues Ser144 to Val1091. Some loop regions are not fully defined by electron density and were not included in the model. The electron density shows an unambiguous binding mode for the ligand, including the orientation and conformation of the ligand. The structure of the complex consists of four domains, including a Ras-binding domain (RBD), a C2 domain, a helical domain, and a catalytic (kinase) domain. The ligand is bound to the kinase domain, which shows the typical bilobal kinase fold with the mainly helical C-terminal lobe and the N-terminal lobe with the β sheet and one important helix. Situated in the cleft formed between the N-terminal and the C-terminal lobe of the kinase domain, the ligand is bound to the ATP binding site and neighboring regions of the active site.

Crystallization and structure determination of lead compound 4 bound to recombinant hPI3Kγ. Expression, purification, and crystallization of hPI3Kγ was performed as described above. Apo-

crystals were used in soaking experiments with compound **4** (1 mM ligand for 2 h followed by 10 mM for 0.5 h). Crystals were flash-frozen and analyzed at a temperature of 100 K. Diffraction data of the complex crystals were collected at the Swiss Light Source (SLS, Villigen, Switzerland) and the structure was solved and refined to a final resolution of 2.88 Å. The crystals contained one monomer of hPI3Kγ in the asymmetric unit and the model comprises residues Ser144 to Val1091. Some loop regions are not fully defined by electron density and were not included in the model. The electron density shows an unambiguous binding mode for the ligand, including the orientation and conformation of the ligand. The structure of the complex consists of four domains, including an RBD, a C2 domain, a helical domain, and a catalytic domain. The ligand is bound to the kinase domain, which shows the typical bilobal kinase fold with the mainly helical C-terminal lobe and the N-terminal lobe with the β sheet and one important helix. Situated in the cleft formed between the N-terminal and the C-terminal lobe of the kinase domain, the ligand is bound to the ATP binding site and neighboring regions of the active site. Based on a distance of <3.5 Å of the donor and acceptor atoms, four specific H-bonds were identified between the ligand **4** and hPI3Kγ, including to the main chain atoms of Val882 and Ala885, as well as the side chain atoms of Lys833.

Associated Contents

Author Information

Corresponding Author

*E-mail: jjeffrey@arcusbio.com

Notes

The authors declare the following competing financial interest(s): All authors are current or former employees of Arcus Biosciences.

Abbreviations Used

AKT, Protein Kinase B; mTOR, Mammalian Target of Rapamycin; Cl_{int}, intrinsic clearance; DMF-DMA, *N*,*N*-dimethylformamide dimethyl acetal; $T_{1/2}$, half-life; HBM, hinge-binding motif; TME, tumor microenvironment; MDSC, myeloid derived suppressor cell; TDI, time-dependent inhibition; NIS,

N-iodosuccinimide; HATU, *N*-[(dimethylamino)-1*H*-1,2,3-triazolo-[4,5-*b*]pyridin-1-ylmethylene]-*N*-methylmethanaminium hexafluorophosphate *N*-oxide; DIPEA, *N*,*N*-diisopropylethylamine.

Accession Codes

Atomic coordinates have been deposited in the Protein Data Bank (https://www.rcsb.org) for PI3Kγ complexed with **4** (PDB ID: 6XRM) and IPI-549 (**3**) (PDB ID: 6XRL). Authors will release the atomic coordinates and experimental data upon article publication.

References

[1] O'Donnell, J. S.; Massi, D.; Teng, M. W. L.; Mandala, M. PI3K-AKT-mTOR inhibition in cancer immunotherapy, redux. *Semin. Cancer Biol.* **2018**, *48*, 91-103.

[2] Thorpe, L. M.; Yuzuguilu, H.; Zhao, J. J. PI3K in cancer: divergent roles of isoforms, modes of action, and therapeutic targeting. *Nat. Rev. Cancer* **2015**, *15*, 7-24.

[3] Yang, J.; Nie, J.; Wei, Y.; Peng, Y.; Wei, X. Targeting PI3K in cancer: mechanisms and advances in clinical trials. *Mol. Cancer* **2019**, *18*, 26.

[4] Hanahan, D.; Weinberg, R. A. The hallmarks of cancer. *Cell* **2000**, *100*, 57-70.

[5] Hanahan, D.; Weinberg, R. A. Hallmarks of cancer: the next generation. *Cell* **2011**, *144*, 646-674.

[6] Fouad, Y. A.; Aanei, C. Revisiting the hallmarks of cancer. *Am. J. Cancer Res.* **2017**, *7*, 1016-1036.

[7] Rodon, J.; Dienstmann, R.; Serra, V.; Tabernero, J. Development of PI3K inhibitors: lessons learned from early clinical trials. *Nat. Rev. Clin. Oncol.* **2013**, *10*, 143-153.

[8] Wang, X.; Ding, J.; Meng, L. PI3K Isoform-selective inhibitors: next-generation targeted cancer therapies. *Acta Pharmacol. Sin.* **2015**, *36*, 1170-1176.

[9] Cushing, T. D.; Metz, D. P.; Whittington, D. A.; McGee, L. R. PI3Kδ and PI3Kγ as targets for autoimmune and inflammatory diseases. *J. Med. Chem.* **2012**, *55*, 8559-8581.

[10] Perry, M. W. D.; Abdulai, R.; Mogemark, M.; Petersen, J.; Thomas, M. J.; Valastro, B.; Eriksson, A. W. Evolution of PI3Kγ and δ inhibitors for inflammatory and autoimmune diseases. *J. Med. Chem.* **2019**, *62*, 4783-4814.

[11] Kaneda, M. M.; Messer, K. S.; Ralainirina, N.; Li, H.; Leem, C. J.; Gorjestani, S.; Woo, G.; Nguyen, A. V.; Figueiredo, C. C.; Foubert, P.; Schmid, M. C.; Pink, M.; Winkler, D. G.; Rausch, M.; Palombella, V. J.; Kutok, J.; McGovern, K.; Frazer, K. A.; Wu, X.; Karin, M.; Sasik, R.; Cohen, E. E. W.; Varner, J. A. PI3Kγ is a molecular switch that controls immune suppression. *Nature* **2016**, *539*, 437-442.

[12] Hirsch, E.; Katanaev, V. L.; Garlanda, C.; Azzolino, O.; Pirola, L.; Silengo, L.; Sozzani, S.; Mantovani, A.; Altruda, F.; Wymann, M. P. Central role for G protein-coupled phosphoinositide 3-kinase γ in inflammation. *Science* **2000**, *287*, 1049-1053.

[13] Davis, R. J.; Moore, E. C.; Clavijo, P. E.; Friedman, J.; Cash, H.; Chen, Z.; Silvin, C.; Van Waes, C.; Allen, C. Anti-PD-L1 Efficacy can be enhanced by inhibition of myeloid derived suppressor cells with a selective inhibitor of PI3Kδ/γ. *Cancer Res*. **2017**, *77*, 2607-2619.

[14] Diaz-Montero, C. M.; Finke, J.; Montero, A. J. Myeloid derived suppressor cells in cancer: therapeutic, predictive, and prognostic indications. *Semin. Oncol.* **2014**, *41*, 174-184.

[15] Gebhardt, C.; Sevko, A.; Jiang, H.; Lichtenberger, R.; Reith, M.; Tarnanidis, K.; Holland-Letz, T.; Umansky, L.; Beckhove, P.; Sucker, A.; Schadendorf, D.; Utikal, J.; Umansky, V. Myeloid cells and related chronic inflammatory factors as novel predictive markers in melanoma treatment with ipilimumab. *Clin. Cancer Res.* **2015**, *21*, 5463-5469.

[16] Trikha, P.; Carson, W. E. Signaling pathways involved in MDSC regulation. *Biochim. Biophys. Acta.* **2014**, *1846*, 55-65.

[17] Evans, C.; Liu, T.; Lescarbeau, A.; Nair, S.; Grenier, L.; Pradeilles, J.; Glenadel, Q.; Tibbitts, T.; Rowley, A.; DiNitto, J.; Brophy, E.; O'Hearn, E.; Ali, J.; Winkler, D.; Goldstein, S.; O'Hearn, P.; Martin, C.; Hoyt, J.; Soglia, J.; Cheung, C.; Pink, M.; Proctor, J.; Palombella, V.; Tremblay, M.; Castro, A. Discovery of a selective phosphoinositide-3-kinase (PI3K)-gamma inhibitor (IPI-549) as an immune-oncology clinical candidate. *ACS Med. Chem. Lett.* **2016**, *7*, 862-867.

[18] Collier, P. N.; Martinez-Botella, G.; Cornebise, M.; Cottrell, K. M.; Doran, J. D.; Griffith, J. P.; Mahajan, S.; Maltais, F.; Moody, C. S.; Huck, E. P.; Wang, T.; Aronov, A. M. Structural basis for isoform selectivity in a class of benzothiazole inhibitors of phosphoinositide 3-kinase γ. *J. Med. Chem.* **2015**, *58*, 517-521.

[19] Collier, P. N.; Messersmith, D.; Le Tiran, A.; Bandarage, U. K.; Boucher, C.; Come, J.; Cottrell, K. M.; Damagnez, V.; Doran, J. D.; Griffith, J. P.; Khare-Pandit, S.; Krueger, E. B.; Ledeboer, M. W.; Ledford, B.; Liao, Y.; Mahajan, S.; Moody, C. S.; Roday, S.; Wang, T.; Xu, J.; Aronov, A. M. Discovery of highly isoform selective thiazolopiperidine inhibitors of phosphoinositide 3-kinase γ. *J. Med. Chem.* **2015**, *58*, 5684-5688.

[20] Come, J. H.; Collier, P. N.; Henderson, J. A.; Pierce, A. C.; Davies, R. J.; Le Tiran, A.; O'Dowd, H.; Bandarage, U. K.; Cao, J.; Deininger, D.; Grey, R.; Krueger, E. B.; Lowe, D. B.; Liang, J.; Liao, Y.; Messersmith, D.; Nanthakumar, S.; Sizensky, E.; Wang, J.; Xu, J.; Chin, E. Y.; Damagnez, V.; Doran, J. D.; Dworakowski, W.; Griffith, J. P.; Jacobs, M. D.; Khare-Pandit, S.; Mahajan, S.; Moody, C. S.; Aronov, A. M. Design and synthesis of a novel series of orally bioavailable, CNS-penetrant, isoform selective phosphoinositide 3-kinase γ (PI3Kγ) inhibitors with potential for the treatment of multiple sclerosis (MS). *J. Med. Chem.* **2018**, *61*, 5245-5256.

[21] Pemberton, N.; Mogemark, M.; Arlbrandt, S.; Bold, P.; Cox, R. J.; Gardelli, C.; Holden, N. S.; Karabelas, K.; Karlsson, J.; Lever, S.; Li, X.; Lindmark, H.; Norberg, M.; Perry, M. W. D.; Petersen, J.; Rodrigo Blomqvist, S.; Thomas, M.; Tyrchan, C.; Westin Eriksson, A.; Zlatoidsky, P.; Öster, L. Discovery of highly isoform selective orally bioavailable phosphoinositide 3-kinase (PI3K)-γ inhibitors. *J. Med. Chem.* **2018**, *61*, 5435-5441.

[22] Gangadhara, G.; Dahl, G.; Bohnacker, T.; Rae, R.; Gunnarsson, J.; Blaho, S.; Öster, L.; Lindmark, H.; Karabelas, K.; Pemberton, N.; Tyrchan, C.; Mogemark, M.; Wymann, M. P.; Williams, R. L.; Perry, M. W. D.; Papavoine, T.; Petersen, J. A class of highly selective inhibitors bind to an active state of PI3Kγ. *Nat. Chem. Biol.* **2019**, *15*, 348-357.

[23] As of April 2020, 93 X-ray crystal structures of human PI3Kγ were contained in the PDB.

[24] Vasta, J. D.; Corona, C. R.; Wilkinson, J.; Zimprich, C. A.; Hartnett, J. R.; Ingold, M. R.; Zimmerman, K.; Machleidt, T.; Kirkland, T. A.; Huwiler, K. G.; Ohana, R. F.; Slater, M.; Otto, P.; Cong, M.; Wells, C. I.; Berger, B.-T.; Hanke, T.; Glas, C.; Ding, K.; Drewry, D. H.; Huber, K. V. M.; Willson, T. M.; Knapp, S.; Müller, S.; Meisenheimer, P. L.; Fan, F.; Wood, K. V.; Robers, M. B. Quantitative, wide-spectrum kinase profiling in live cells for assessing the effect of cellular ATP on target engagement. *Cell Chem. Biol.* **2018**, *25*, 206-214.

[25] Furet, P.; Guagnano, V.; Fairhurst, R. A.; Imbach-Weese, P.; Bruce, I.; Knapp, M.; Fritsch, C.; Blasco, F.; Blanz, J.; Aichholz, R.; Hamon, J.; Fabbro, D.; Caravatti, G. Discovery of NVP-BYL719 a potent and selective phosphatidylinositol-3 kinase alpha inhibitor selected for clinical evaluation. *Bioorg. Med. Chem. Lett.* **2013**, *23*, 3741-3748.

[26] Knight, Z. A.; Gonzalez, B.; Feldman, M. E.; Zunder, E. R.; Goldenberg, D. D.; Williams, O.; Loewith, R.; Stokoe, D.; Balla, A.; Toth, B.; Balla, T.; Weiss, W. A.; Williams, R. L.; Shokat, K. M. A Pharmacological map of the PI3-K family defines a role for p110α in insulin signaling. *Cell* **2006**, *125*, 733-747.

[27] Berndt, A.; Miller, S.; Williams, O.; Le, D. D.; Houseman, B. T.; Pacold, J. I.; Gorrec, F.; Hon, W.-C.; Ren, P.; Liu, Y.; Rommel, C.; Gaillard, P.; Rückle, T.; Schwarz, M. K.; Shokat, K. M.; Shaw, J. P.; Williams, R. L. The P110δ structure: mechanisms for selectivity and potency of new PI(3)K inhibitors. *Nat. Chem. Biol.* **2010**, *6*, 11-124.

[28] Somoza, J. R.; Koditek, D.; Villaseñor, A. G.; Novikov, N.; Wong, M. H.; Liclican, A.; Xing, W.; Lagpacan, L.; Wang, R.; Schultz, B. E.; Papalia, G. A.; Samuel, D.; Lad, L.; McGrath, M. E. Structural, biochemical, and biophysical characterization of idelalisib binding to phosphoinositide 3-kinase d. *J. Biol. Chem.* **2015**, *290*, 8439-8446.

[29] Yasuhara, A.; Kameda, M.; Sakamoto, T. Selective monodesulfonylation of *N,N*-disulfonylarylamines with tetrabutylammonium fluoride. *Chem. Pharm. Bull.* **1999**, *47*, 809-812.

Table of Contents Graphic